



Review Article

Bed-parallel slip associated with normal fault systems

Efstratios Delogkos ^{*}, Vincent Roche ^{*}, John J. Walsh ^{*}*Fault Analysis Group and iCRAG (Irish Centre for Research in Applied Geosciences), UCD School of Earth Sciences, University College Dublin, Belfield, Dublin, Ireland*

ARTICLE INFO

Keywords:
Bed-parallel slip
Normal faults
Extensional tectonics
Multilayer sequence

ABSTRACT

Stretching of the Earth's upper crust is commonly accommodated by normal faulting, fault-related folding and/or fracturing such as veins and joints. However, an increasing number of outcrop-scale studies highlight that extension is also accompanied by bed-parallel slip (BPS). The identification of BPS surfaces is, however, challenging due to their localised nature within bedded host rock sequences, the absence of suitable slip markers, and the scale and resolution of both outcrop and seismic reflection data. Here, we present examples of BPS identified within extensional fault systems in sedimentary sequences and outline the nature, magnitude, segmentation, and spatiotemporal distribution of BPS surfaces. These constraints provide a basis for defining the principal structural controls on BPS development and its geometric and kinematic relationship to normal faulting. We conclude that BPS is a common feature within multi-layered host rock sequences, irrespective of their lithological and mechanical properties, and is kinematically associated with a broad range of fault-related deformation, including bed rotations, flexural-slip folding, and both tectonic and gravity-driven sliding. The presence of BPS within normal fault systems can increase the complexity of the host rock volumes and fracture arrays with potential implications on subsurface fluid flow and seismicity.

1. Introduction

Upper crustal extension of layered sequences in sedimentary basins is usually accommodated by a combination of localised discontinuous deformation (faulting and fracturing) and continuous deformation (folding), with the latter often involving a combination of flexural-slip and flexural-flow folding. Whilst the prevalence of brittle deformation processes at shallow to moderate crustal depths is widely recognised, the importance of localised slip along bedding, i.e., bed-parallel slip (BPS), is not. In this study we investigate the nature of BPS within multilayer sequences in extensional tectonic regimes, developing upon previous studies on similar processes and structures, including layer-parallel slip, bedding-parallel fault, flexural-slip fault, layer-parallel shear or bed-parallel shear (e.g., Chapple and Spang, 1974; Salehy et al., 1977; Higgs et al., 1991; Gross et al., 1997; Ferrill et al., 1998; Li et al., 2015; Lemonnier et al., 2020).

BPS has long been recognised and extensively investigated in compressional tectonic regimes. In fold and thrust belts, in particular, layer parallel shortening is accommodated by ramp-flat thrust systems (e.g., Rich, 1934; Sanderson, 1982; Eisenstadt and De Paor, 1987) and associated flexural-slip and flexural-flow folding (e.g., Ramsay, 1974; Tanner, 1989; Horne and Culshaw, 2001; Ishii, 2016). The importance

of BPS is promoted by the moderate deformation depths of fold and thrust belts (< ca. 10 km), and by the low angle between mechanical layering and sub-horizontal shortening, a scenario which favours slip localisation along bedding.

By contrast, in regions subjected to extension, BPS is less often considered to be an intrinsic component of accommodating deformation. During the last decade, however, there has been an increasing number of studies describing BPS associated with normal faulting (e.g., Weinberger et al., 2016; Delogkos et al., 2017, 2018; Laubach et al., 2018; Alsop et al., 2020; Lemonnier et al., 2020; Nabavi et al., 2020), and supporting the importance and abundance of BPS in extensional tectonic settings. In this study, we provide an overview of the origin and nature of BPS associated with normal fault systems, outlining the geometrical and kinematic relationships between the BPS planes and normal faults, on the one hand, and the magnitude of slip and spatio-temporal distribution of BPS planes, on the other. This review concentrates on conventional rift systems with low-moderate basin extensions, and does not consider more highly extended crustal systems comprising the shallow-dipping rotated faults and regionally extensive detachments, including those developed in association with metamorphic core complexes and continental hyperextension (e.g., Carmignani and Kligfield, 1990; Peacock et al., 2000; Ye et al., 2022).

* Corresponding authors at: School of Earth Sciences, University College Dublin, Belfield, Dublin 4, Ireland.

E-mail addresses: stratos.delogkos@ucd.ie (E. Delogkos), vincent.roche@ucd.ie (V. Roche), john.walsh@ucd.ie (J.J. Walsh).

Table 1

Database of bed-parallel slip identified in extensional settings.

Location	Proposed BPS origin (see Figs. 1 and 3)	Lithology	Data type	Min BPS (m)	Max BPS (m)	Configuration (see Fig. 2)	Figure in the paper	Reference
Dead Sea Basin, Israel	Flexural-slip due to fault propagation folding	Intercalated shale, gypsum, and dolostone	Outcrop	Na	Na	(a), (c)	Fig. 4a	Gross et al., 1997
Suez Rift, Egypt	Flexural-slip due to fault propagation folding	Limestone, sandstone, mudstone, and conglomerate	Outcrop	Na	Na	(a), (b), (c-d)	Fig. 4b	Sharp et al., 2000; Jackson et al., 2006; Wilson et al., 2009
Northern Red Sea, Egypt	Flexural-slip due to fault propagation folding	Shale, limestone, and sandstone	Outcrop	Na	Na	Na	Na	Khalil and McClay, 2017
Ramon National Geological Park, Israel	Flexural-slip due to fault propagation folding	Limestone, sandstone, marl, clay and chalk	Outcrop	Na	Na	(a), (b)	Na	Becker, 1994
Sierra Del Carmen, Texas, USA	Flexural-slip due to fault propagation folding	Limestone and shale	Outcrop	0.28	0.71	(c)	Na	Ferrill et al., 2007; Smart et al., 2010
Analogue sandbox experiment	Flexural-slip due to fault propagation folding	Multilayer clay	Experiment	Na	Na	(a), (c)	Na	Withjack et al., 1990
Gubbio normal fault, Italy	Flexural-slip due to fault-bend folding	Limestone and mudstone	Outcrop	0.07	0.15	(b)	Na	Benedicto and Schultz, 2010
Buckskin Mountains, Arizona, USA	Flexural-slip due to fault-bend folding	Sandstone and siltstone	Outcrop	Na	Na	(a)	Fig. 4c	Laubach et al., 2018
Kilve, Somerset, England, UK	Flexural-slip due to fault-related folding	Limestone, shale, and mudstone	Outcrop	Na	1.5	(c)	Fig. 6d	This study
Kato Zakros, Crete, Greece	Flexural-slip due to fault-related folding	Sandstone and shale	Outcrop	0.35	0.95	(c), (c-d)	Figs 6c, 7a	This study
Glacier National Park, Montana, USA	Flexural-slip due to hanging-wall rollover anticline	Limestone and shale	Outcrop	0	0.9	(a), (b), (c)	Fig. 5a	Higgs et al., 1991
Sevier Fault, Utah, USA	Flexural-slip due to hanging-wall rollover anticline	Interbedded mudstones and sandstones	Outcrop	0.01	0.4	(b) and (c)	Na	Higgs et al., 1991
Ptolemais Basin, Greece	Flexural-slip due to hanging-wall rollover anticline	Lignite and marl	Outcrop	0.07	4.5	(a), (b), (c), (c-d)	Figs 4d, 7c	Delogkos et al., 2017, 2018; Childs et al., 2020
Huércal-Overa Basin, Spain	Flexural-slip either hanging-wall rollover anticline or fault-bend folding	Conglomerate, sandstone, and siltstone	Outcrop	Na	Na	(a)	Na	Pedrera et al., 2012
Arches National Park, Utah, USA	Flexural-slip due to chevron hanging-wall syncline	Sandstone and shale	Outcrop	Na	3	(b), (c)	Na	Watterson et al., 1998
Moab fault, Utah, USA	Flexural-slip due to undefined fault-related folding	Sandstone and shale	Outcrop	Na	0.5	(c), (c-d)	Na	Ferrill et al., 2009
Asturian Basin, Spain	Flexural-slip due to undefined fault-related folding	Limestones, shales, marl, dolostones and mudstones	Outcrop	Na	0.1	(a), (b)	Na	Granado et al., 2018
Northumberland, England, UK	Flexural-slip due to undefined fault-related folding	Limestone, sandstone, coal, and clay	Outcrop	0	1	(c), (c-d)	Na	Salehy et al., 1977
Dead Sea Basin, Israel	Gravity-driven downslope movement	Aragonite and detrital-rich layers	Outcrop	0.04	0.95	(a), (c)	Fig. 6a	Alsop et al., 2020
Ierapetra Basin, Crete, Greece	Gravity-driven downslope movement	Sandstone, marl, clay, breccia, and conglomerate	Outcrop	Na	Na	(a), (c)	Na	Gamboa and Alves, 2015
Brazil, Espírito Santo Basin	Gravity-driven downslope movement	Open marine sequence	Seismic	Na	Na	(a), (c)	Na	Gamboa and Alves, 2015
Kii Mountains, Japan	Gravity-driven downslope movement	Shale and sandstone	Borehole	Na	Na	Na	Na	Chigira et al., 2013
Thandwe Beach, Myanmar	Gravity-driven downslope movement	Turbidites	Outcrop	Na	Na	(a)	Na	Morley, 2014
Guayllabamba, Ecuador	Gravity-driven downslope movement	Volcaniclastic sediments	Outcrop	0.05	1	(c)	Fig. 6f	Personal communication with Carlos Giraldo
Dead Sea Basin, Israel	Simple-shear due to co-seismic shaking	Aragonite and detrital-rich layers	Outcrop	0.05	0.6	(c)	Na	Weinberger et al., 2016
Zanjan Depression, Iran	Simple shear due to rotated beds between slip-surfaces	Marl, silt, conglomerate, sandstone, and alluvium units	Outcrop	Na	0.3	(b), (c), (c-d)	Fig. 5b	Nabavi et al., 2020
				Na	Na	(b)	Fig. 5c	Watterson et al., 1998

(continued on next page)

Table 1 (continued)

Location	Proposed BPS origin (see Figs. 1 and 3)	Lithology	Data type	Min BPS (m)	Max BPS (m)	Configuration (see Fig. 2)	Figure in the paper	Reference
Brider Jack Mesa, Utah, USA	Simple shear due to rotated beds between slip-surfaces	Dominantly eolian sandstones						
Round O Quarry, Lancashire, England, UK	Simple shear due to rotated beds between slip-surfaces	Sandstone and shale	Outcrop	0.01	0.8	(b), (c), (c-d)	Fig. 5d	Watterson et al., 1998
Lodeve basin, France	Simple shear due to rotated beds between slip-surfaces	Sandstone and shale	Outcrop	Na	0.2	(b)	Na	Wibberley et al., 2007; van der Zee et al., 2008
Bare Mountain, Nevada, USA	Tectonic movement, tilted multilayer sequence	Limestones and dolomites with intercalated silty and sandy beds	Outcrop	Na	0.1	(c)	Fig. 6b	Ferrill et al., 1998
Sorbas Basin, Spain	Tectonic movement, tilted multilayer sequence	Conglomerate, sandstone, mudstone, and siltstone sequence	Outcrop	Na	1	(a), (c), (c-d)	Na	Andrić et al., 2018
Sagres, Portugal	Tectonic movement, tilted multilayer sequence	Turbidites	Outcrop	Na	4	(c)	Na	Fossen, 2020
Grès d'Annot, France	Tectonic movement, tilted multilayer sequence	Deep-water siliciclastic deposits	Outcrop	Na	Na	(a), (b)	Na	Lansigu and Bouroulec, 2004
Lodeve basin, France	Tectonic movement, tilted multilayer sequence	Shale and sandstone	Outcrop	0.1	3	(b), (c), (c-d)	Na	Wibberley et al., 2007; van der Zee et al., 2008
Aigion Fault, Greece	Undefined fault related	Turbiditic deep marine carbonates	Borehole	Na	Na	(a)	Na	Daniel et al., 2004
Inner Moray Firth, North Sea, UK	Unknown	Unknown	Seismic	Na	300	(c-d)	Fig. 11	Iacopini et al., 2016
Brider Jack Mesa, Utah, USA	Unknown	Sandstone and mudstone	Outcrop	Na	0.1	(c)	Fig. 6g	This study
Courthouse, Utah, USA	Unknown	Sandstone and mudstone	Outcrop	Na	0.2	(c)	Fig. 6e	This study
Watchet, Somerset, England, UK	Unknown	Limestones interbedded with shales	Outcrop	Na	Na	Na	Na	Hancock, 1985
Gargano Promontory, Italy	Unknown	Limestone and chert sequence	Outcrop	Na	0.5	(c)	Na	Korneva et al., 2016
Vocontian trough, France	Unknown	Limestone and shale	Outcrop	Na	Na	(a)	Na	Roche et al., 2012; Roche et al., 2017; Lemonnier et al., 2020
Ardeche margin, France	Unknown	Limestone and shale	Outcrop	Na	Na	(a)	Fig. 4e	Roche et al., 2012; Roche et al., 2017; Lemonnier et al., 2020
Northumberland and Durham Coalfield, England, UK	Unknown	Coal, mudstone, siltstone, sandstone, and clay	Outcrop	Na	Na	Na	Na	Stimpson and Walton, 1970

Since the early work by [Anderson \(1905\)](#), it has been long known that normal, thrust and strike-slip faults can often be distinguished by the geometries, slip directions and orientations of associated, sometimes conjugate, faults. By contrast, BPS planes have a geometry that is intrinsically controlled by mechanical layering, with their formation arising from local stress conditions and bed-parallel localisation rather than simply reflecting the far-field tectonic setting under which they formed. Consequently, it can be challenging to identify the origin of BPS, in particular in regions that have had a polyphase tectonic history (e.g., [Séjourné et al., 2005; Lemonnier et al., 2020](#)). In this study, we provide a basis for defining the origins of BPS and shedding light on the challenges of interpreting BPS.

By comparison to dip-slip normal faults offsetting shallow-dipping sedimentary layers, identification of BPS is often difficult due to the bed-parallel nature of BPS and the paucity of offset markers. In some instances, BPS planes can be diagnosed from associated microstructures such as slickenlines, shear veins, fault rock and/or mineralisation, either from outcrop or well data (e.g., [Ferrill et al., 2007; Weinberger et al., 2016; Lemonnier et al., 2020](#)), but in many others these may not be identifiable and/or present (e.g., [Delogkos et al., 2017, 2018; Alsop et al., 2020; Nabavi et al., 2020](#)). BPS planes may, therefore, remain invisible in the absence of other displaced markers such as faults, veins

or joints that are oblique to bedding. For these reasons, recognition of BPS from seismic reflection data is not straightforward because the displaced markers and BPS planes are likely to be below the limit of seismic resolution. This review of the characteristics and various contexts of BPS is intended to provide constraints on the occurrence and development of BPS in extensional settings. We suggest that together with faults, veins, and joints, BPS planes are fundamental and prevalent discontinuities within deformed rock volumes. Not only are they a key component of how deformation is partitioned, they can also affect fluid flow (e.g., [Couples et al., 1998; Gamboa and Alves, 2015](#)) and seismicity (e.g., [Shaw and Suppe, 1994; Gutiérrez et al., 2014](#)) within basins. Our synthesis of the interaction of normal faults and BPS is intended to shed light on geometrical aspects of associated fault/fracture systems, and their implications for fracturing, seismicity, and fluid flow linked to numerous associated applications, such as radioactive waste disposal, carbon storage, hydrocarbon production and fluid injection operations.

Previous accounts of BPS in extensional settings are here compiled in a database which comprises 43 different study areas worldwide ([Table 1](#)). Most of the previous studies were primarily aimed at investigating normal fault geometry, with BPS identified and described in that context. This review provides an overview of the geometric and kinematic relationships between the BPS and normal faulting (Section

2), the mechanical conditions required for BPS in extensional settings (Section 3), the structural controls on its development (Section 4), and the magnitude, segmentation, and spatiotemporal distribution of the BPS planes (Section 5). We mainly focus on BPS studies from outcrop data where BPS is best observed, but also provide examples of BPS investigated from other types of data such as borehole, experimental and seismic reflection data.

2. Geometric and kinematic relationships between bed-parallel slip and normal faulting

Bed-parallel slip within an extensional fault system is often found to be geometrically and/or kinematically associated with normal faulting (Figs. 1, 2 and 3). In this section, we explore the four main

configurations identified in the literature between normal faulting and BPS (Fig. 2), as a backdrop to later considerations of the origin and structural controls on their formation.

2.1. Normal faults abutting BPS

There are several accounts of normal faults abutting BPS planes in the published literature (Table 1; Figs. 1a, b and 2a). In this configuration, normal faults are bounded vertically by the BPS surface(s) without being displaced by them (see selected examples in Fig. 4), a relationship suggesting that faults are mechanically linked to or retarded by BPS. Numerous studies have identified examples of spatially constrained arrays of normal faults accommodating displacement transfer between BPS planes. In this case, BPS are the primary structures, with the

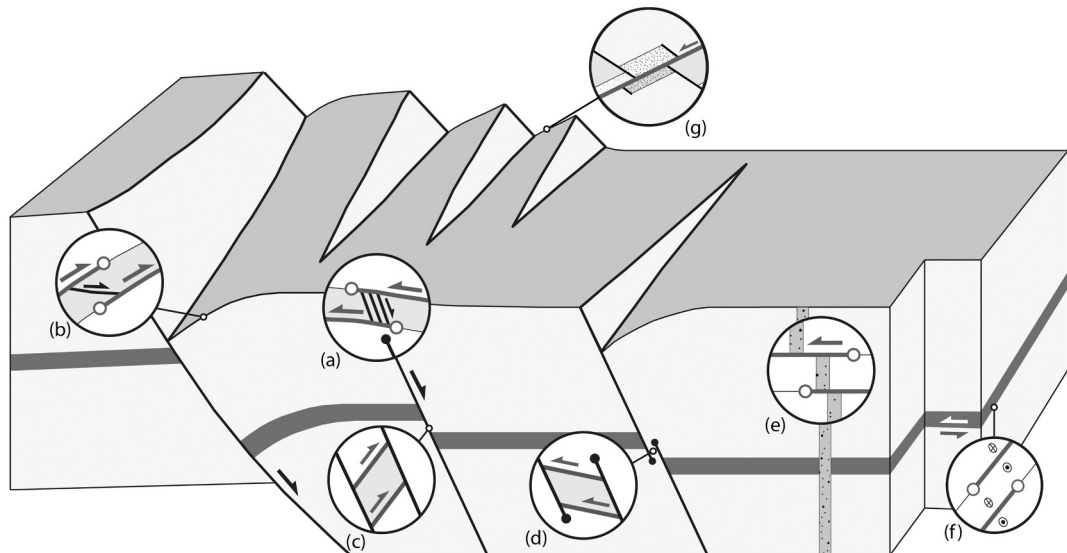


Fig. 1. Conceptual block diagram illustrating the different origins and segmented nature of BPS within an extensional fault system. (a) BPS due to flexural-slip associated with fault-propagation folding (e.g., Fig. 3a). (b) BPS due to flexural-slip associated with rollover at the hanging-wall of a master fault (e.g., Fig. 3b). The BPS planes in (a) and (b) are segmented parallel to the slip direction forming domino-style faults (a) and a releasing relay zone with a “connecting” normal fault (b) to accommodate slip transfer. (c) and (d) BPS due to simple shear associated with synthetic and antithetic bed rotations, respectively, between interacting faults (e.g., Fig. 3c and d). (e) BPS due to simple shear associated with co-seismic shaking (e.g., Fig. 3f). The displaced marker in this case is a clastic dike. The BPS plane is segmented parallel to the slip direction forming a restraining relay zone. (f) Segmented BPS plane normal to the slip direction forming a neutral relay zone. (g) BPS due to either tectonic movement along favourable rotated bed interfaces or gravity-driven downslope movement (e.g., Fig. 3e).

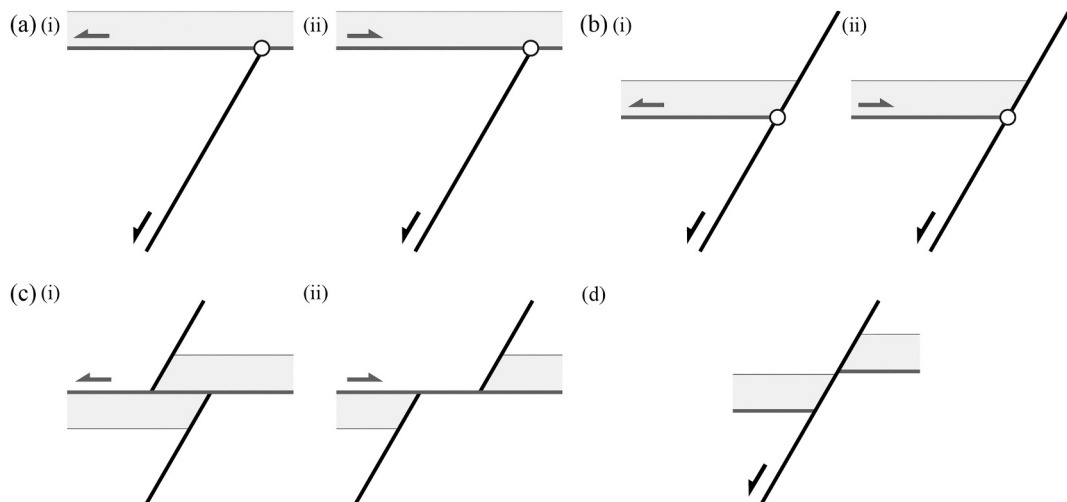


Fig. 2. The geometric and/or kinematic relationships between BPS and normal faulting. (a) Normal fault abutting BPS plane. (b) BPS abutting normal fault. (c) BPS offsetting normal fault. (d) Normal fault offsetting BPS plane. Two scenarios are shown for configurations (a) to (c), in which the sense of slip on the BPS plane and fault are either the same (i) or different (ii).

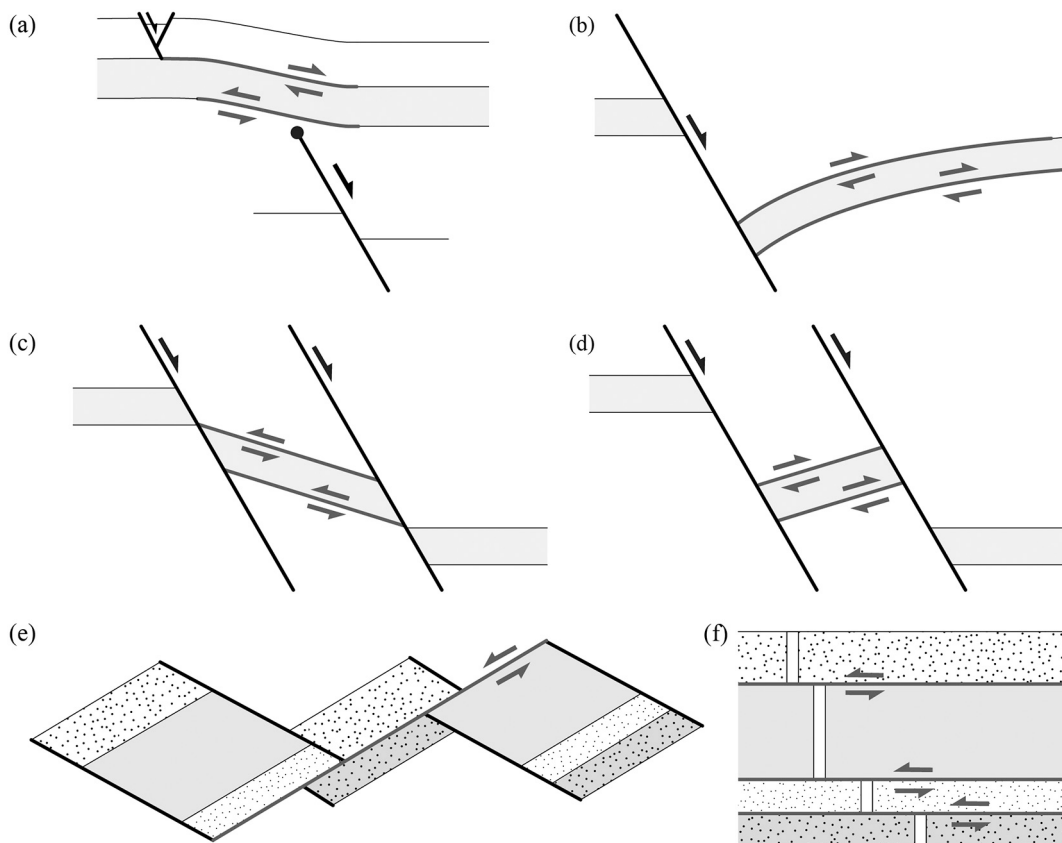


Fig. 3. Origins of BPS within an extensional fault system. (a) and (b) Flexural-slip driven BPS associated with fault-propagation folding (a) and rollover at the hanging-wall of a master fault (b). (c) and (d) BPS due to simple shear associated with synthetic (c) or antithetic (d) bed rotation between interacting fault surfaces. (e) Tectonic movement along favourable rotated bed interfaces (modified after Ferrill et al., 1998) or gravity-driven downslope movement. (f) BPS due to simple shear associated with co-seismic shaking. The displaced marker in this case is a clastic dike.

orientation and displacement of the normal faults governed by the direction and the magnitude of BPS, respectively. For example, Gross et al. (1997) described normal faults that are directly linked to BPS planes associated with flexural-slip folding in the Dead Sea rift (Figs. 1a, b, 4a). Delogkos et al. (2018) identified releasing relay zones and associated domino-style faults (e.g., antithetic to the overall sense of BPS) and “connecting” normal faults (e.g., synthetic to the overall sense of BPS) that, together with the upper and lower BPS planes, form extensional duplexes exposed in intercalated lignite and marl deposits in the Ptolemais Basin (NW Greece) (Figs. 1a, b and 4d). Pedrera et al. (2012) described similar configurations in alternating sandy and silt layers in the Huércal-Overa Basin (SE Spain) where minor normal faults bounded by BPS planes are interpreted to be part of a releasing overstep zone that eventually forms an extensional duplex structure.

Further examples of normal faults abutting BPS planes have been described by Roche et al. (2012, 2017) in alternating clay-rich and limestone layers exposed in the Mesozoic South-Eastern Basin of France (Fig. 4e). These studies also provided insights into the displacement evolution along the normal faults, which propagated and then abutted BPS planes while continued accumulating displacement resulting in high normal fault displacement gradients, a mechanism referred to as restriction by the authors. Microstructural analyses of the BPS planes in the same study areas have shown that BPS recorded successive tectonic events, which are expressed by recurrent crack-seal veins, pull-apart veins and stylolites (Lemonnier et al., 2020). In contrast, the BPS planes in Ptolemais Basin described by Delogkos et al. (2018) were not marked by associated fault rock or related mineral fill.

2.2. BPS abutting normal faults

Kinematic interaction between normal faulting and BPS can lead to a configuration where BPS planes are bounded laterally by normal fault(s) but without being displaced by them (Table 1; Figs. 1c, d and 2b). Examples of this configuration are provided in Fig. 5, including syn-kinematic BPS planes within tilted strata abutting against two synthetic bounding normal faults exposed in the Plio-Quaternary sedimentary series of the Zanjan Depression, Iran (Fig. 5b; Nabavi et al., 2020). A similar abutting relationship has been observed for strong synthetic rotation (i.e., down towards the hanging-wall) of beds and associated BPS planes within a strongly deformed narrow fault zone, with bounding normal faults accommodating a much larger throw (~120 m) along a fault near Moab, Utah, USA (Fig. 5c; Watterson et al., 1998). The associated space problem at fault-BPS plane intersections can be accommodated in other ways. For example, abutting contacts between synthetic rotated BPS planes and a normal fault are shown in Fig. 5d, where a straight footwall slip surface of the normal fault is separated from the overhanging steps on hanging-wall slip surface by a 15–30 cm thick shaly fault gouge at Round O Quarry, Lancashire, UK (Watterson et al., 1998).

2.3. BPS offsetting normal faults

Identifying BPS within extensional fault systems is challenging in the absence of appropriate offset markers such as faults (e.g., Alsop et al., 2020), veins (e.g., Ferrill et al., 2007), and dykes (e.g., Weinberger et al., 2016). When BPS offsets pre-existing structures, the resulting geometry is much simpler for veins and dykes (e.g., Figs. 1e and 3f), because they do not offset the layering to provide the complexity of structure

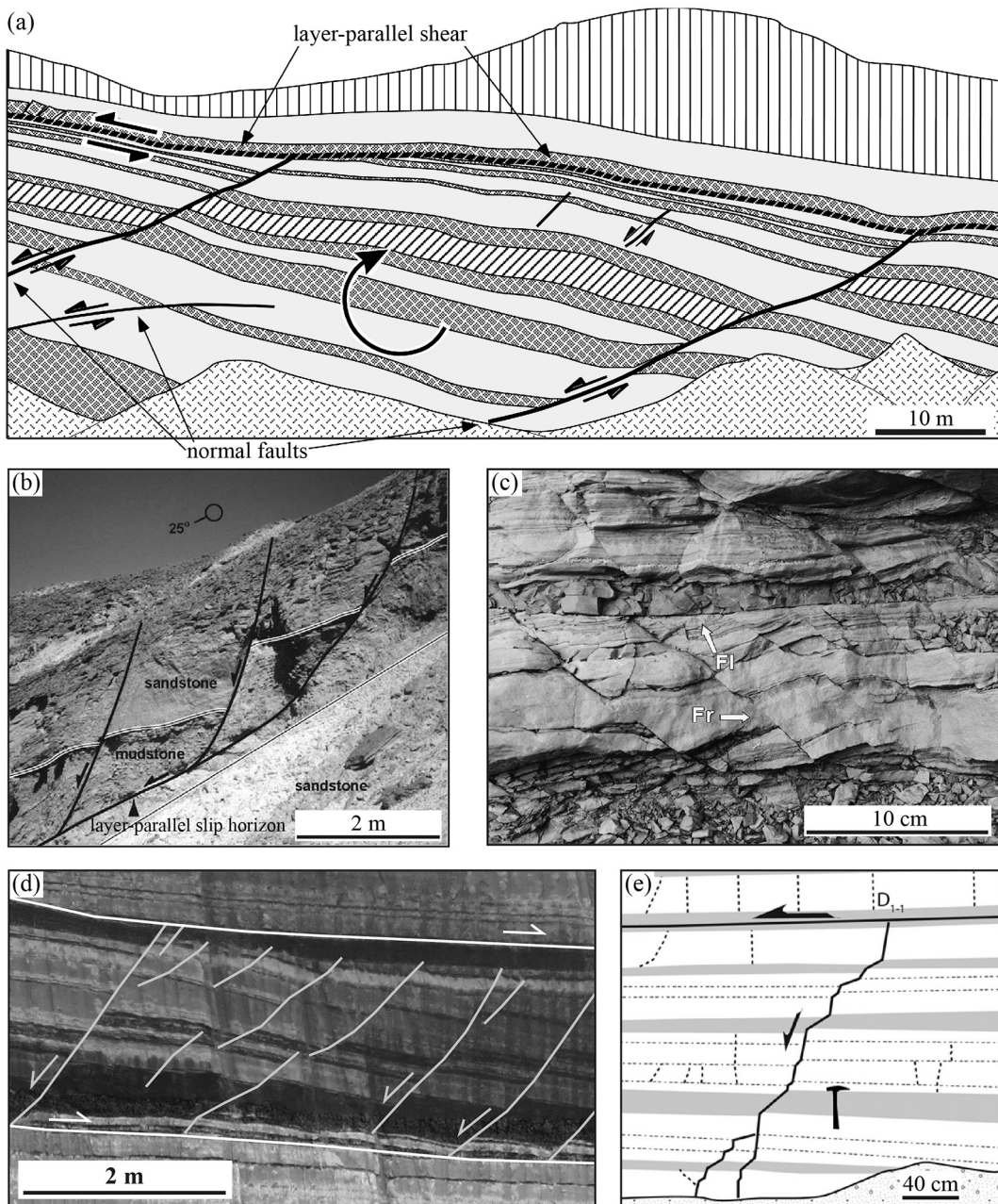


Fig. 4. Outcrop examples where a normal fault abuts at BPS plane. (a) BPS associated with a monoclinal structure above a basement bounding normal fault in the Dead Sea Basin (after Gross et al., 1997). (b) Normal faults detaching downwards onto a BPS mudstone horizon in the Suez Rift (after Jackson et al., 2006). (c) Subparallel normal faults (Fr) bounded by flat fault (Fl) in western Arizona (after Laubach et al., 2018). (d) Bookshelf-style faulting related to the BPS in the Ptolemais Basin, Greece (after Delogkos et al., 2018). (e) Normal fault abuts at BPS plane in the South-Eastern Basin, France (after Roche et al., 2017).

sometimes accompanying normal faulting (Figs. 1g and 2c). An example of the former has been identified by Weinberger et al. (2016) in the Dead Sea Basin, in which vertical clastic dykes are displaced by BPS planes within a very shallow (<15 m) sequence consisting of aragonite and detrital-rich layers. In this case, a 1-m-thick shear zone consisting of up to 11 BPS planes with displacements of up to 60 cm on individual slip surfaces is attributed to near-surface deformation of a multilayer sequence during a single earthquake event.

Offset of normal faults by BPS results in their segmentation and the formation of extensional (Fig. 2c(i)) or contractional (Fig. 2c(ii)) steps depending on the direction of BPS relative to the dip direction of the displaced normal fault. Particularly, when BPS displaces normal faults with a synthetic sense of movement (Figs. 2c(i), 6c, 6d and 6f), a stepped 'sawtooth' pattern is developed and part of the stratigraphic sequence is

repeated, with older over younger stratigraphic relationships across the BPS plane (Delogkos et al., 2017; Alsop et al., 2020; Nabavi et al., 2020). In contrast, when BPS displaces a normal fault with an antithetic sense of movement (Figs. 2c(ii), 6a, 6b, 6e, 6f and 6g), a stepped 'staircase' pattern is developed, and part of the stratigraphic sequence is missing with younger over older stratigraphic relationships across the BPS plane. In both cases, the throw of the normal fault at the time of the BPS event can be estimated as it equals the thickness of the repeated or missing part of the stratigraphic sequence (Fig. 2c).

2.4. Normal faults offsetting BPS

Because normal faults are abundant and long-lived structures, the configuration of normal faulting offsetting BPS planes is expected to be

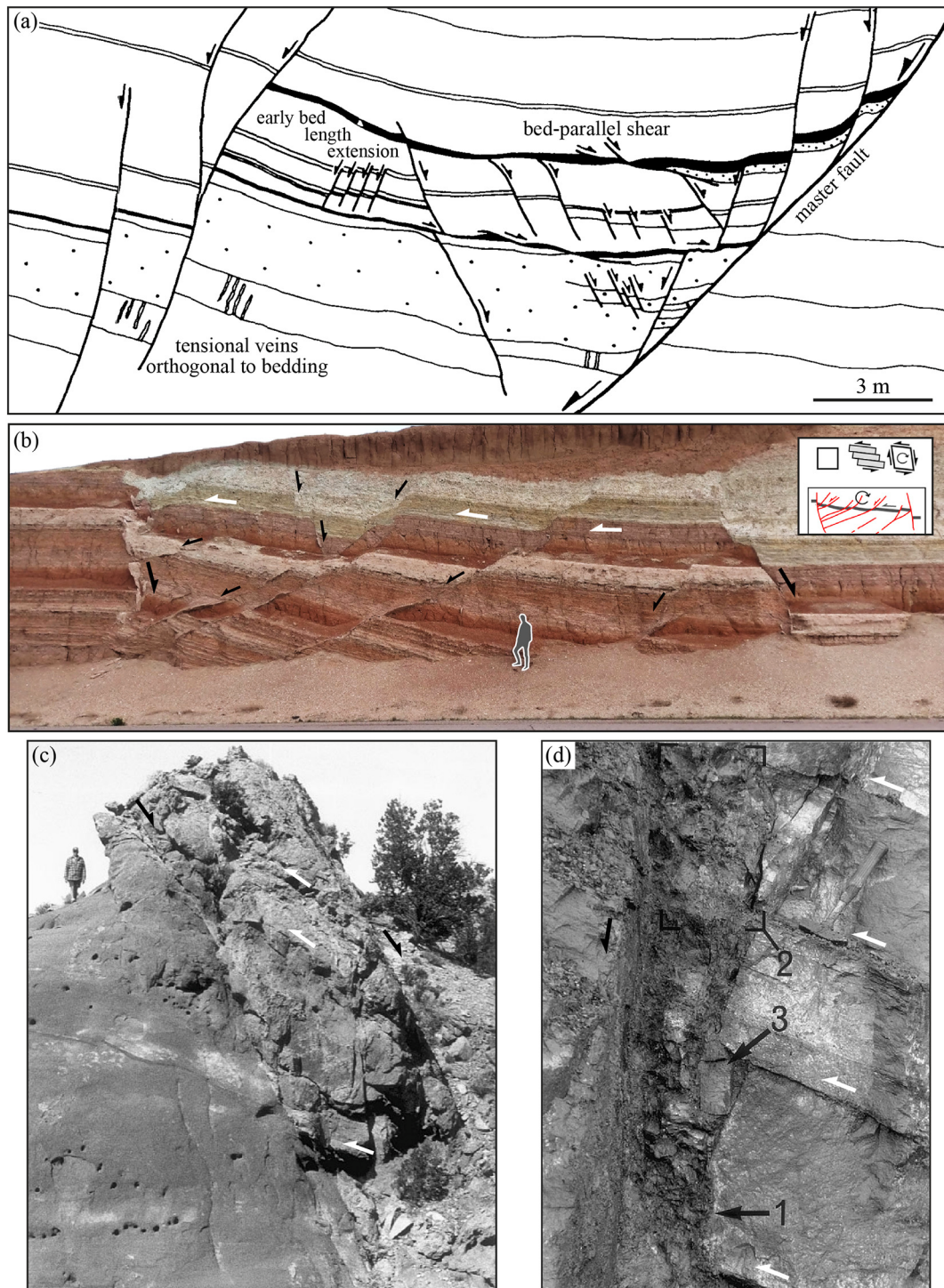


Fig. 5. Outcrop examples where BPS abuts at normal fault. (a) A normal fault system exposed in the Glacier National Park, Montana, USA (after Higgs et al., 1991). (b) Normal fault zone enclosing a series of antithetic normal faults accompanying tilting of the strata and *syn-kinematic* BPS in the Zanjan Depression, Iran (after Nabavi et al., 2020). (c) Normal fault zone with sharply defined external slip surfaces enclosing uniformly rotated beds at Bridger Jack Mesa, near Moab, Utah, USA (after Watterson et al., 1998). (d) A 210-cm-displacement fault zone with footwall (left) separated from hanging-wall (right) by 15–30 cm of shaly fault gouge containing sandstone blocks of various sizes at Round O Quarry, Lancashire, UK (after Watterson et al., 1998).

the most common (Fig. 2d). However, due to the difficulty of identifying the presence of BPS planes in the absence of suitable pre-existing offset markers (i.e., faults and veins), clear evidence of normal faults offsetting BPS planes (Fig. 2d) has only been established in cases of multiple repetitions of normal faulting and BPS (Fig. 7). For example, Delogkos et al. (2017) demonstrated that BPS planes in Ptolemais Basin, NW Greece, were displaced several times by normal faults during their

reactivation following offset by BPS. As expected, the resulted geometry at the intersection area between mutually offsetting BPS planes and normal faults is complicated. Fig. 7a illustrates one of these examples where a normal fault was initially displaced by BPS when its throw was ca. 1.5 m as indicated by the thickness of the repeated section within the fault zone. Subsequent reactivation of the normal fault resulted in the propagation of both, the upper and lower, fault segments, offset of the

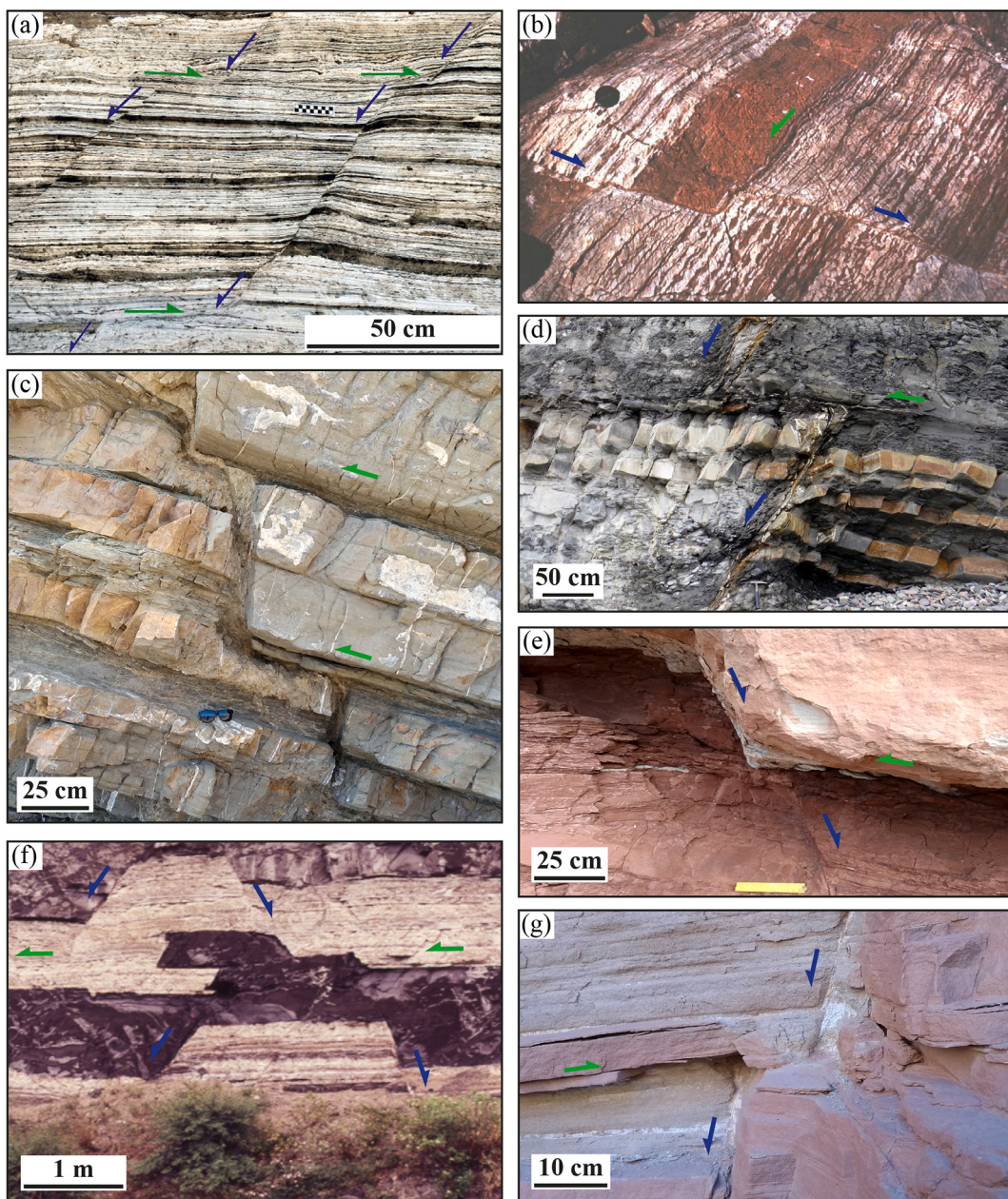


Fig. 6. Outcrop examples where BPS offsets normal fault exposed in the (a) Dead Sea Basin (after Alsop et al., 2020), (b) Bare Mountain, Nevada, USA (after Ferrill et al., 1998), (c) Kato Zakros, Eastern Crete, Greece, (d) Kilve, UK, (e) Courthouse, Utah, USA, (f) Guayllabamba, Ecuador (photo courtesy of Carlos Giraldo), and (g) Bridger Jack Mesa, Utah, USA.

pre-existing BPS planes and the formation of a fault-bounded lens. A simpler case is shown in Fig. 7b where subsequent reactivation of the normal fault resulted in reactivation and propagation of only the lower fault segment and offset of the hanging-wall BPS plane (green layer). The triangular blocks in Fig. 7c represent former underhanging steps formed by BPS and subsequent reactivation of the initially planar fault slip surface (Watterson et al., 1998).

3. Mechanical conditions required for BPS in extensional settings

Our compilation of previous studies reveals that BPS can have a variety of origins in extensional settings (Table 1), which are summarised in Figs. 1 and 3. They comprise: (i) flexural-slip associated with fault-related folding (Figs. 1a, b, 3a and b), (ii) simple shear associated

with bed rotation (Figs. 1c, d, 3c and d), (iii) tectonic movement along favourable rotated bed interfaces (Figs. 1g and 3e), (iv) gravity-driven downslope movement (Figs. 1g, 3a and e), and (v) co-seismic shaking (Figs. 1e and 3f). Here we provide a brief consideration of the mechanical conditions required for BPS in extensional settings, as a backdrop to a more detailed description of each of those origins in the next section.

In an extensional regime, the maximum far-field principal stress is vertical. Depending on the magnitudes of the effective stresses, fracturing under this regime typically produces three different types of fractures: (i) vertical fractures opening normal to the minimum principal stress due to tensile failure, (ii) 60°–70° dipping normal faults due to compressional shear failure, and (iii) hybrid fractures with differing amounts of dilation formed under a mixed tensile and compressive stress state (e.g., Hancock, 1985; Ramsey and Chester, 2004; Ferrill et al.,

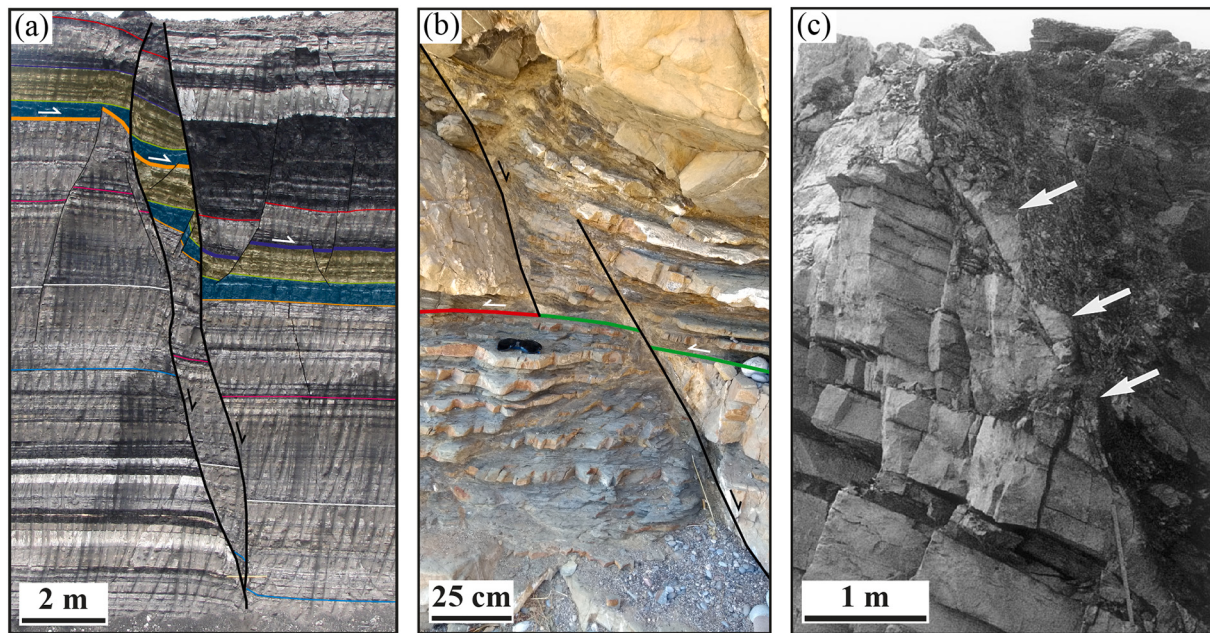


Fig. 7. Outcrop examples where normal fault offsets BPS plane. (a) A 5.5 m throw normal fault zone in Ptolemais Basin, Greece (after Delogkos et al., 2017). The fault was displaced by BPS when the throw was equal to the repeated colour filled part of the sequence within the fault zone. Subsequent fault movement resulted in reactivation of both segments of the offset fault which in turn offset the BPS plane. (b) A normal fault which was affected by BPS during its growth in Kato Zakros, Eastern Crete, Greece. Subsequent reactivation of the normal fault after the BPS resulted in upward propagation of the lower fault segment and offset of the BPS plane (green). (c) A 5-m-displacement fault zone with triangular blocks (arrowed) separated from footwall and displaced from their source beds along the straight footwall slip surface at Round O Quarry, Lancashire, UK (after Watterson et al., 1998). (For interpretation of the references to colour in this figure legend, the reader is referred to the web version of this article.)

2012a, 2012b; Fig. 8a). In this context, the development of BPS in strata that are moderate to shallowly dipping (i.e., < 50°) involves shearing at a high angle to the maximum far-field principal stress and appears to be inconsistent with the expectations of classic fracture mechanics. Although determination of the exact stress conditions producing individual cases of BPS is not possible, there are several factors which can together contribute to BPS formation, the most important of which are: (1) strength anisotropy coupled with bed rotation, (2) stress rotation, and (3) fluid overpressure.

BPS is typically encountered within foliated and stratified anisotropic rocks where the strength properties parallel to bedding are likely weaker than in other directions (i.e., low friction and cohesion). Laboratory tests demonstrate that in extensional stress conditions slip can occur along surfaces with dips as low as 30° with transecting normal faults only dominating when anisotropies have dips shallower than ca. 30° (e.g., Donath, 1961; Niandou et al., 1997; Khanlari et al., 2015; Fig. 8b). Consequently, within extensional basins, in which the maximum principal stress is vertical, mechanically anisotropic sequences with moderate-steep bed dips (>30°) will be prone to BPS. While this mechanism alone may explain some examples of BPS (see Section 4.4), in other cases departures of the maximum principal stress from vertical can promote BPS initiation even at lower bed dips. These circumstances will apply when the deformation of bedded sequences is accommodated locally by the partitioning of pure or simple shear components that are oblique to the far-field stresses. For example, flexural-slip folding associated with normal faulting (Figs. 1a, b and 8c; see Section 4.1) and the deformation of host rock sequences within fault zones and relays (Fig. 1c and d) in which a combination of simple shear and pure shear, arising from bed rotation and associated fault zone narrowing, provides a local stress field that can be rotated to very high angles relative to the far-field (Fig. 8d and e; Sanderson and Manchini, 1984; see Section 4.2). Arising from these rotations bedding can accommodate the slips predicted along equivalent conjugate faults within the prevailing stress orientations (Fig. 8f). Lastly, fluid

overpressure may further decrease the angle of stability of bedding by partly supporting overburden pressures and reducing the frictional resistance of the bedding planes as fluid pressures approach lithostatic (Hubbert and Rubey, 1959; Healy, 2009). The development of overpressures within basinal sequences typically occurs when compaction-related pressures cannot be dissipated by fluid flow, particularly within low permeability units, such as shales and clays. These circumstances will facilitate BPS, sometimes with the generation of BPS-dominated gravitational sliding (Cobbold et al., 2004; see Section 4.3). The foregoing discussion indicates, therefore, that a variety of conditions that are relatively common within layered basinal sequences can promote the formation of BPS associated with normal faulting, a suggestion which is developed further in the next section.

4. Structural controls on the development of BPS

The foregoing section has outlined some of the main factors relating to the prevailing stress conditions associated with BPS in extensional settings. Despite the apparent paradox of combining normal faults and BPS, these considerations highlight how normal faulting within sedimentary basins will inevitably be accompanied by BPS. In this section we investigate some of the associated processes in more detail.

4.1. Flexural-slip folding

Flexural-slip is a deformation mechanism that has been widely applied in compressional settings for accommodating folds in layered sequences through the initiation of *syn*-folding slip along bedding planes (Ramsay, 1974; Tanner, 1989). Outcrop analysis of BPS associated with flexural-slip folding has shown: (a) a correlation between the fold style parameters (e.g., fold curvature, shape, interlimb angle) and the amount of slip, (b) a systematic change in the magnitude of flexural-slip from a maximum along the fold limb to zero at the fold hinges and (c) bedding slip directions (defined from slickenlines and slickenfibres) are near

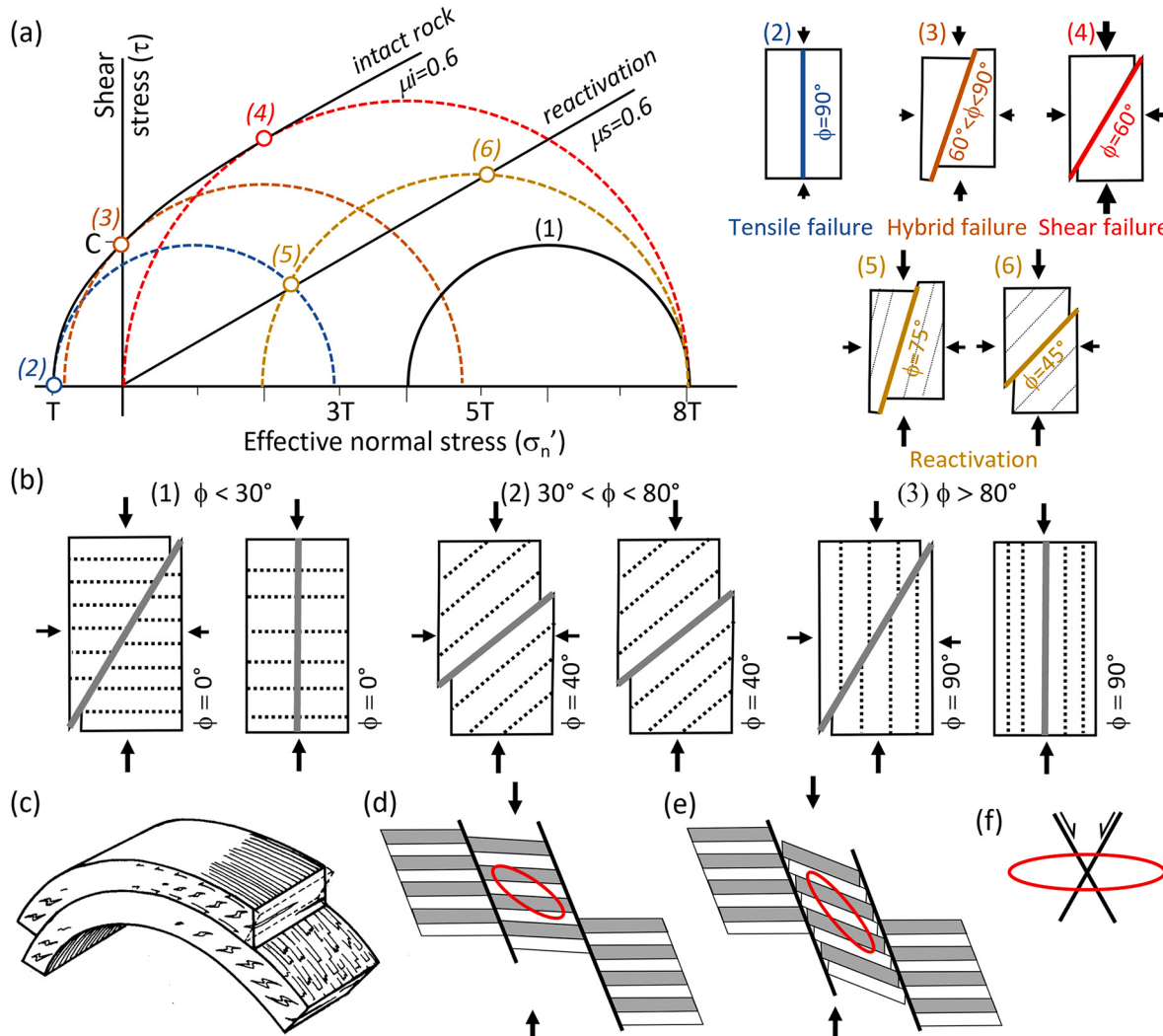


Fig. 8. (a) Mohr diagram of shear stress, τ , against effective normal stress, σ_n' illustrating the different modes of failure for an intact homogeneous rock with a composite Griffith-Coulomb failure envelope and the reactivation of cohesionless pre-existing faults with a straight failure envelope (modified from Hancock, 1985 and Sibson, 2000). C is tensile strength and T is cohesion. Coefficient of internal friction (μ_i) and friction coefficient (μ_s) of pre-existing faults is 0.6. Initial stress condition (1) before the effect of increased fluid pressure or tectonic loading. Tensile (2), hybrid (3) and shear failures (4) as the stress magnitudes are modified. Stress conditions for the reactivation of cohesionless pre-existing faults, which are misoriented at $\phi = 75^\circ$ (5) and $\phi = 45^\circ$ (6). (b) Failure modes in anisotropic rocks due to the presence of planes of weakness (dashed lines; modified from Niandou et al., 1997). Shear and tensile failure occurring across bedding for bed dips (1) $\phi < 30^\circ$, (2) $30^\circ \leq \phi < 80^\circ$, and (3) $\phi \geq 80^\circ$ at low and high confining stress, respectively. (c) Flexural-slip fold, with slickenfibres along BPS planes and tension gashes within competent layers formed by layer-parallel shearing (Price and Cosgrove, 1990). (d) and (e) Fault zone bounded by two slip-surfaces showing the infinitesimal strain ellipses (red) for simple shear with no shortening (d) and for simple shear with ca. 10% shortening (e). (f) Orientation of conjugate faults relative to infinitesimal strain ellipse assuming a coefficient of internal friction of 0.6 (same as (3) in (a)). (For interpretation of the references to colour in this figure legend, the reader is referred to the web version of this article.)

orthogonal to the fold hinge and, in the absence of overturned bedding, have a reverse sense of shear that changes across the fold hinges (Tanner, 1989, 1992; Suppe, 1985; Fowler, 1996; Fagereng and Byrnes, 2015; Séjourné et al., 2005).

Flexural-slip folding is the principal origin of bed-parallel slip identified in extensional tectonic settings (Table 1). Among the different forms of folding that can exist in extensional settings (e.g., Hamblin, 1965; Shelton, 1984; Barnett et al., 1987; Walsh and Watterson, 1987; Withjack et al., 1990; Gawthorpe et al., 1997; Sharp et al., 2000; Grasemann et al., 2005; Childs et al., 2017; Rowan et al., 2020), fault-propagation folds (Fig. 3a) are most often reported to accommodate BPS (Table 1). In this case, folds with axes sub-parallel to fault strike develop above the upper tip, or in some cases below the lower tip, of a propagating normal fault (e.g., Barnett et al., 1987; Grasemann et al., 2005; Ferrill et al., 2007; Childs et al., 2017; Coleman et al., 2019). These folds are also considered to be the precursory deformation

responsible for the presence of normal drag directly adjacent to a normal fault (e.g., Walsh and Watterson, 1987; Grasemann et al., 2005; Ferrill et al., 2012a, 2012b) suggesting the potential presence of BPS associated with normal drag. An example of BPS associated with fault-propagation folding in Sierra Del Carmen Mountain range in west Texas, USA, has been analysed in detail by Ferrill et al. (2007). In this case a monocline is developed above a propagating normal fault with a displacement on the order of 100–500 m (Fig. 9a). The folded limestone and shale sequence includes bed-perpendicular veins accommodating bed-parallel extension, and a series of BPS planes with an up-dip sense of shear offsetting the veins with a maximum displacement of 63 cm. These deformation features are mostly concentrated in the monoclinal limb, where the maximum intensity of flexural-slip folding is expected (Fig. 9a). Further increase of the displacement and propagation of the underlying normal fault can eventually result in breaching of the fold (e.g., Sharp et al., 2000), making it difficult to identify the presence and origin of BPS.

BPS associated with flexural-slip folding has also been attributed to hanging-wall rollover anticlines (Table 1; Fig. 3b), a reverse drag feature associated with both planar and listric faults (e.g., Hamblin, 1965; Shelton, 1984; Barnett et al., 1987; Stein et al., 1988). Delogkos et al. (2018) examined the nature of BPS arising from a hanging-wall rollover anticline on a km-scale displacement normal fault in Ptolemais Basin, NW Greece. In this case, flexural-slip along the hanging-wall rollover was accommodated by 78 BPS planes with an up-dip sense of movement that can be observed within the 110 m of exposed stratigraphic sequence composed mainly from alternations of relatively thin lignite and marl beds. A previous study by Watterson et al. (1998) provided estimations of the contribution that wall-rock steps arising from BPS due to hanging-wall rollover anticlines may have on fault rock thickness.

The characteristic feature of the flexural-slip models already presented is BPS with an up-dip sense of shear, but there are other models which generate down-dip shear. For example, based on analogue models aiming to replicate fault propagation folding, Withjack et al. (1990) described a folded multilayer sequence above a normal fault that has been affected by BPS with two opposed senses of shearing. In this case, one BPS plane has an up-dip sense of movement which is attributed to the flexural-slip folding (i.e., lower BPS plane in Fig. 3a), while the other BPS plane has a down-dip sense of shear which is attributed to have a tectonic origin by accommodating lateral transfer of extension (i.e., upper BPS plane in Fig. 3a). This lateral transfer of extension is also accommodated by secondary high-angle normal faults which are located upslope, above the BPS plane and are connected to it (e.g., Fig. 3a). Natural examples of BPS planes with a down-dip sense of shear within fault-propagation folds have also been identified by Sharp et al. (2000) and Jackson et al. (2006) in the *syn-* and pre-rift sequences in the Suez Rift, Egypt (Fig. 4b).

In his classic study of listric faults with detachments, Gibbs (1984) highlighted that antithetic faults located at the hanging-wall rollover can detach on bedding surfaces and, therefore, generate a down-dip sense of BPS, which is in contrast with the flexural-slip mechanism that has an up-dip sense of movement. Another example of a down-dip sense of BPS associated with hanging-wall rollover anticlines attributed to listric faults has been identified by Higgs et al. (1991) within the Sevier fault system in southwestern Utah, USA. These authors did not attribute this contrasting sense of movement to a tectonic or a gravitational origin (see Sections 4.2 and 4.3), but to a different flexural-slip mechanism that assumes the extensional fault plane acts as the finite neutral surface of the fold, with associated bed-parallel slip extending well beyond the associated hanging-wall rollover anticline, a boundary condition we consider geometrically unlikely. The associated down-dip sense of movement contrasts with the up-dip sense arising from more conventional models involving conservation of bed length and thickness within the hanging-wall block and pinning of the beds at the outer limit of the hanging-wall rollover (Rowan and Kligfield, 1989; Watterson et al., 1998; Delogkos et al., 2018).

4.2. Simple shear associated with bed rotations between interacting faults

Simple shear is a deformation in which the parallel planes of a translated body remain parallel and maintain a constant distance, while translating relative to each other (e.g., Ramsay, 1980). In the case of two parallel interacting fault slip surfaces, the shear movements on the faults result in rotation of the beds and associated bed-parallel slip with up-dip movements between the bounding faults (Fig. 3c and d). The bed rotation can be associated with either synthetic or antithetic bed rotations between kinematically interacting parallel fault surfaces, i.e., see Fig. 3c and d, respectively. The shear between bounding fault surfaces can lead to local stresses with very different orientations to those of the far-field, circumstances which can strongly favour the localisation of BPS (Fig. 8d and e). The resulting structure has been described by Watterson et al. (1998), as similar to a kink-band but without the same geometric constraints, as the bounding faults effectively provide free surfaces.

Watterson et al. (1998) provided outcrop examples of BPS accommodating shear between closely spaced interacting faults suggesting that, in this case, BPS, which is associated with the bed rotations, contributes to the transfer of displacement between the bounding fault surfaces (Figs. 3c, d and 5c). A recent study by Nabavi et al. (2020) has also shown an outcrop example of *syn-kinematic* BPS related to synthetic tilting of the strata within a vertically segmented normal fault zone (Fig. 5b). In these cases, the space problems associated with abutting BPS and normal faults, will be accommodated by a variety of deformation mechanisms, including cataclastic and plastic flow of host rocks and/or faults rocks, pressure solution and veining, depending on the lithological properties of the host rock sequence and the boundary conditions.

The simple shear model and the flexural-slip model discussed previously are both related to bed rotations that result in an up-dip sense of bed-parallel slip. These two models can therefore be difficult to distinguish. However, according to Watterson et al. (1998), their main difference is on the slip distribution along the BPS planes which is discussed in detail in Section 5.3.

4.3. Gravity-driven movement

BPS associated with gravity-driven normal faulting (Fig. 3e) occurs when downslope shear movement is activated on rotated bedding planes due to gravitational forces. Gravity-driven BPS has been widely recognised in mass-transport deposits, in which a strong association with normal faulting characterises the extension-dominated upslope region of such systems (e.g., Bull et al., 2009). Aspects of the formation and kinematics of mass-transport deposits and the associated basal shear surfaces have been well described from both seismic reflection and outcrop data (e.g., Bull et al., 2009; Alsop and Marco, 2011; Sobiesiak et al., 2018), with recent studies (Table 1) identifying the development of internal BPS planes. For example, Gamboa and Alves (2015) integrated observations from a 3D seismic reflection dataset from SE Brazil, and outcrop data from SE Crete, Greece, and demonstrated that BPS can develop within mass-transport blocks during their downslope movement, with important potential implications for internal fluid flow pathways. Evidence of BPS within mass-transport deposits can sometimes also be provided by borehole data, with, for example, BPS identified down to depths of 86 m within gravitationally deformed shales and sandstones in onshore Japan (Chigira et al., 2013). Detailed field analysis of BPS within mass-transport deposits along the western margin of the Dead Sea Basin (Alsop et al., 2020), has indicated the prevalence of multiple internal BPS planes with displacements of up to tens of centimetres and a characteristic downslope movement towards the depocenter of the basin (Fig. 6a). This study highlighted that whilst BPS planes may have limited displacements, their cumulative effects within the mass-transport deposits have significant implications for the accommodation and estimation of extension and contraction within gravity-driven systems. Because BPS due to gravity-driven downslope movements is associated with slope instabilities, the prevalence of this deformation will vary with location and depth, with its development expected to be accentuated at shallower burial depths within basin margins. Identification of BPS with a downslope sense of movement does not, however, require that deformation is gravity-driven, since it could also have a tectonic-driven origin (see Section 4.4).

4.4. Post-rotation BPS localisation

As we have shown in Section 3, bed-parallel slip can be promoted by the tilting of bedding planes so that they are activated as slip surfaces due to their favourable orientation relative to the local or far-field stresses (Fig. 3e). This process of activation is sensitive to orientations and relative magnitudes of the principal stresses and to the mechanical properties of the faulted sequence (e.g., Ferrill et al., 1998). BPS due to tectonic or gravity-driven movement are both likely to have a downslope

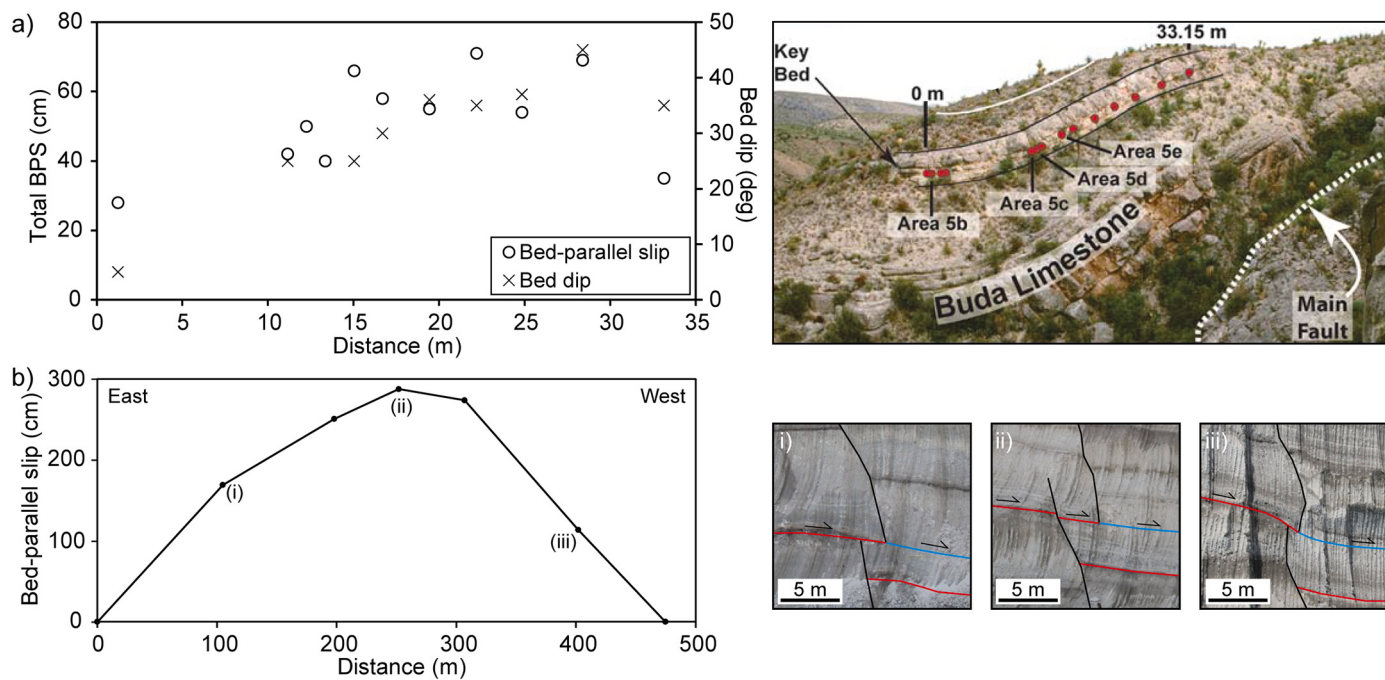


Fig. 9. (a) Total bed-parallel slip (circles, scale on left side) and key bed dip (crosses, scale on right side) plotted versus measured distance along a single limestone layer in the Buda Limestone exposed in Sierra Del Carmen, Texas, USA (outcrop on the right; after Ferrill et al., 2007). (b) Bed-parallel slip profile normal to the slip direction based on measurements along a normal fault which is displaced by BPS in Ptolemais Basin, Greece (see the outcrops on the right) after Delogkos et al. (2018).

sense of movement. However, while gravitational driven BPS is expected at shallow depths (see Section 4.3), tectonic activation of bedding planes can also be expected at greater depths depending on the frictional properties of the bedding planes and the magnitude of the driven stresses (e.g., Morris et al., 1996; Ferrill et al., 1998). Tectonic activation of BPS has been proposed by Ferrill et al. (1998) to explain BPS observed at Bare Mountain, Nevada, USA (Fig. 6b). In this case, fault blocks provide bedding planes that are progressively rotated until BPS is initiated due to the higher slip tendency of bedding planes, arising from the increasing obliquity with the maximum principal stress direction. Activation of the bedding planes as slip surfaces has also been reported in tilted Carboniferous turbidites during Triassic rift-related faulting in Sagres, Portugal (Fossen, 2020).

Beyond these two examples, we speculate that activation of bedding planes as slip surfaces is also possible in areas of high crustal stretching. Existing models for crustal stretching envisage progressive extension along fault systems generally involving rotating fault blocks down-thrown towards the locus of crustal thinning. In these circumstances existing models suggest that the progressively lower dips of normal faults, and an associated increase in normal stress (σ_n), leads to their deactivation and the generation of a newly formed set of steeper faults (e.g., Proffett Jr, 1977; Jackson, 1987; Reston, 2005). Whilst these newly formed faults are also generally considered to dip in the same direction as the earlier set of faults, the earlier rotation of bedding within fault blocks will provide anisotropy that dips at angles greater than the rotations of original faults. For the high crustal stretching factor (β) values typical of stretched crust approaching the generation of oceanic crust (e.g., $\beta = 2-3$) bed rotations in excess of 45° are to be expected, circumstances which will make the activation of bedding planes as slip surfaces (e.g., generation of opposed dipping faults) more favourable than the generation of new synthetic faults (see also Section 3). This will lead to the generation of a conjugate fault system as crustal stretching proceeds, a scenario that is envisaged in some crustal stretching models (Bayrakci et al., 2016; Lymer et al., 2019).

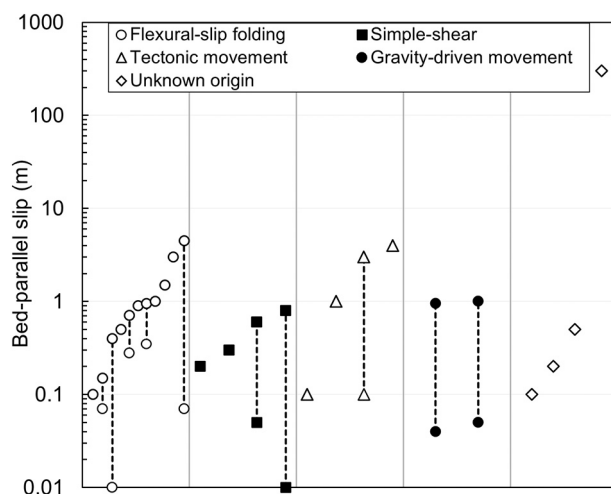


Fig. 10. Maximum and where possible minimum magnitude of BPS categorised by its origin. Each datapoint represents a different study area (for more details see Table 1).

4.5. Simple shear associated with co-seismic shaking

BPS can also be related to horizontal simple shear associated with co-seismic shaking (Fig. 3f). To the best of our knowledge, the only account of BPS formed due to co-seismic shaking in extensional settings has been identified by Weinberger et al. (2016) in the Dead Sea Basin. In this case, vertical clastic dykes are displaced by BPS planes within a very shallow (<15 m) sequence consisting of aragonite and detrital-rich layers. A 1-m-thick shear zone consisting of up to 11 BPS planes with displacements of up to 60 cm on individual slip surfaces is attributed to a single co-seismic event. Weinberger et al. (2016) suggested that BPS can accommodate co-seismic shaking, a scenario that can be promoted at shallow depths in a multilayer sequence where enhanced tensile stresses and lower vertical stresses (σ_1) can lead to mechanical decoupling along

bedding planes and gravity sliding.

5. Magnitude, segmentation, and distribution of bed-parallel slip

5.1. Magnitude of bed-parallel slip

The magnitude of BPS typically ranges from a few millimetres up to a few meters, and is of the same order for all different origins of BPS associated with normal fault systems (Fig. 10; Table 1). We recognise, however, that our compiled quantitative dataset, which mainly comprises data from outcrop datasets (Table 1), is subject to a sampling bias that limits the range of observed magnitudes of BPS, the nature of which is discussed further in this section.

Even in outcrop exposures where detailed observations can be made, identifying and measuring BPS can often be challenging. In the absence of steep-vertical markers, faults are much easier to observe within sedimentary sequences and because they are the pre-eminent driver of associated structures (e.g., folds and BPS), their kinematics are easier to define and unravel than the smaller and more enigmatic BPS. In addition, faults will often transect and offset BPS planes, making them even more challenging to recognise (see Section 2.4). For example, analysis of BPS from the Ptolemais Basin benefits from large-scale open-cast mine exposures supporting the localised nature of BPS with m-scale slips, which are metres to decametres apart (Delogkos et al., 2017, 2018; Childs et al., 2020). Even in that area the presence of BPS remained elusive for the first couple of years during the mapping of fault zone structure, only becoming clear because of the remarkable stratigraphic definition of the faulted sequence and the absence of cataclasis and fault rock generation destroying fault-BPS contacts within unlithified host rocks deformed at relatively shallow depths of faulting (< ca. 200 m). Without those conditions identifying BPS will be very difficult in normal fault-BPS systems where faults are the principal structures both in terms of their displacement and longevity, and where contemporaneous BPS must step across contemporaneous faults. Similar conclusions were derived from the analysis of gravity slides within the Dead Sea rift, with Alsop et al. (2020) suggesting that based on their inability to correlate

the displaced markers at outcrop scale, BPS planes could potentially have magnitudes in the order of 10's metres, potentially with multiple BPS planes complicating the estimation of extension and/or contraction in gravity-driven systems.

A potential means of investigating larger-scale BPS is from the analysis of seismic reflection data, but those data are arguably subject to even more significant resolution effects. For example, even fault zones accommodating 1 km scale displacements do not have sufficient content to be imaged seismically and are only mappable from offset horizons. It is therefore expected that BPS, which are likely to be intrinsically localised and do not offset horizons, will be even more challenging to identify. Despite these concerns, the presence of BPS from seismic reflection data of submarine mass-transport deposits in offshore Espírito Santo, SE Brazil, has been advocated by Gamboa and Alves (2015), although their magnitude was not defined. Here we present an interpreted seismic line of a potential example of BPS associated with a normal fault system in the Inner Moray Firth, North Sea (Fig. 11; Iacopini et al., 2016). Although it has not been proposed by the authors, this interpretation suggests the presence of large-scale BPS. On first inspection this fault looks like a cross-section of a conventional relay zone, in which the pair of fault surfaces at the lower part of the section could be bounding structures to a breached relay zone seen in map view (e.g., Peacock and Sanderson, 1991; Childs et al., 1995, 1996). However, closer examination of the interpreted seismic line highlights the key geometric characteristics associated with fault segmentation due to BPS (Delogkos et al., 2017). For example, the displacement gradients at the tips of the relay bounding fault segments are infinite, especially for the hanging-wall fault segment that juxtaposes the yellow unit (Fig. 11). This is accompanied by repetition of part of the stratigraphic sequence (i.e., the red unit in Fig. 11), with associated abrupt changes in the displacement gradients at the bounding fault segments. Following BPS, it also appears that the footwall fault segment was reactivated and propagated upwards displacing the BPS surface. Based on this interpretation, the estimated magnitude of BPS in this case is ca. 300 m which equals the separation distance between apparent relay bounding fault segments. Detailed restorations of very similar geometries of alternating normal faulting and bed-parallel slip have been presented by Delogkos

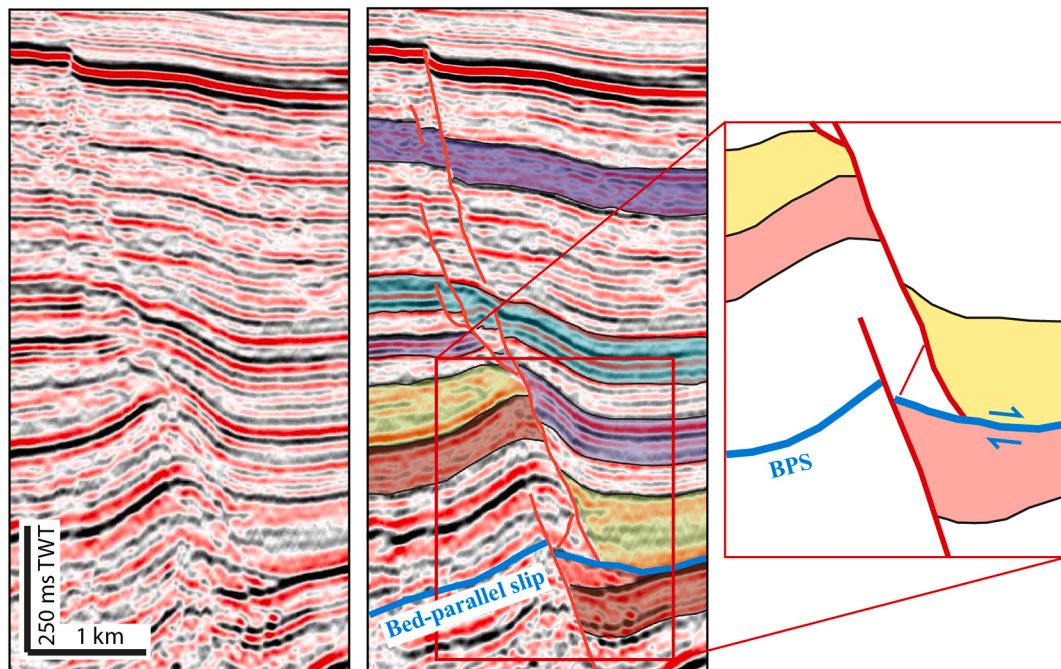


Fig. 11. Non-interpreted and interpreted seismic image of a normal fault zone in Inner Moray Firth, North Sea. (modified after Iacopini et al., 2016; see also the Virtual Seismic Atlas).

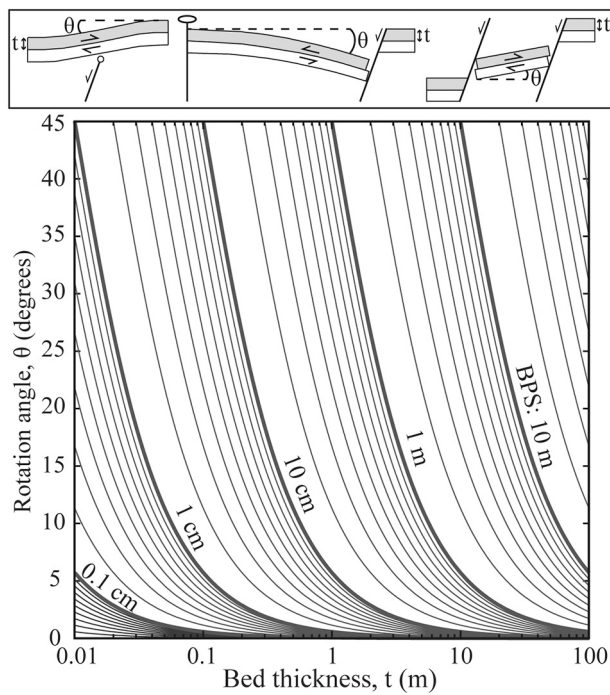


Fig. 12. Graph showing the modelled relationship between the magnitude of bed-parallel slip (BPS), the average bed thickness (t), and the rotation angle (θ) of the beds associated with either flexural-slip, associated with fault propagation folding (top-left) or hanging-wall rollover anticline (top-centre), or simple shear, associated with bed rotations between interacting faults (top-right).

et al. (2017) for meter-scale, outcrop-based examples. Whilst we anticipate that future analysis will highlight the presence of intermediate BPS magnitudes, between this seismic example and those of our outcrop datasets (e.g., > 4.5 m and < 300 m; Fig. 10), their identification might be challenging due to the limitations in scale and resolution of both data sources.

5.2. Relationship between BPS, bed rotation and bed thickness

A quantitative consideration of the magnitude of BPS can be performed by comparing empirical constraints derived from a selection of datasets with conceptual models of BPS. A sense of the scale of BPS associated with faults can be defined for simple geometric models of the structural controls we described in Section 4, including flexural-slip associated with both fault propagation folds or hanging-wall rollover anticlines, and simple shear arising from bed rotations between interacting faults. For simplicity, we investigate models with sequences

assumed to have constant bed thickness and equally spaced BPS surfaces, with angular bed rotations measured from a horizontal regional (Fig. 12). Whilst in practice natural multi-layered sequences are likely to be marked by BPS which varies with bed thickness and with the properties of potential slip surfaces, the simple models presented give a sense of the scale of slip relative to bed thickness and rotations. Estimated BPS are considered maxima because no account is taken of bed rotations accommodated by other, more ductile, processes in natural systems (e.g., compaction, pressure solution, buckling). Results are presented for bed thicknesses from 1 cm up to 100 m and for bed dips of up to 45°, which exceeds the ca. 20° maximum bed dips for all but two of the natural examples presented in this paper (Fig. 12). These exceptions are relatively high strain examples of a fault propagation fold, the Big Brushy Canyon monocline, adjacent to a 75 m displacement normal fault (Fig. 9) within the West Texas extensional corridor (Ferrill et al., 2007) and a fault zone along Bridger Jack Mesa fault (Fig. 5c), a 120 m displacement normal fault within the Paradox Basin, Utah. For both the flexure and simple shear models there is a linear relationship between BPS and bed thickness for a constant bed rotation angle, and between BPS and bed rotation angle for a constant bed thickness, such that

$$s = \tan(\theta)^* t \quad (1)$$

Fig. 12 shows the magnitude of BPS (s) on individual bedding planes within a multilayer sequence with bed thicknesses (t) and rotations (θ). Thick bedded sequences (1–10 m) will have BPS of ca. 0.3–3 m for bed dips of up to 20°, and 0.1–1 m for bed dips up to 5°, whilst thin bedded sequences (<10 cm) will have BPS of <4 cm for 20° bed dips and <1 cm for 5° bed dips. The range of BPS values compares well with those expected for the bed dips and bed thicknesses in the examples presented in this review, though the lowest BPS values predicted are slightly lower than those observed. We attribute this difference to two principal effects, the difficulty of confidently defining cm-scale BPS given the complex structure of combined fault-BPS systems and the likelihood that there will not be an equivalence between bed thickness and the spacing of BPS (see also Sections 5.5 and 5.6). The latter arises from the fact that only selected bedding planes are likely to become the locus for slip and some will accommodate more slip than others, an established feature of fracture localisation within other systems (Kakimi, 1980; Wojtal, 1986; Childs et al., 1990; Gillespie et al., 1993). Whilst the rather limited range of BPS (a few centimetres up to 4.5 m) in natural systems is attributed to sampling bias and localisation, the observational constraints are nevertheless in line with the simple models presented. This is illustrated for a single dataset of a fault-propagation fold investigated by Ferrill et al. (2007) in which BPS was measured for different bed dips across a hanging-wall monocline (Fig. 9a). Correlation between bed dip and BPS is consistent with flexural slip decreasing towards fold hinges and increasing towards steepened limbs. This change was defined by measuring the slip-thickness ratio of BPS-bed thickness pairs, a measure

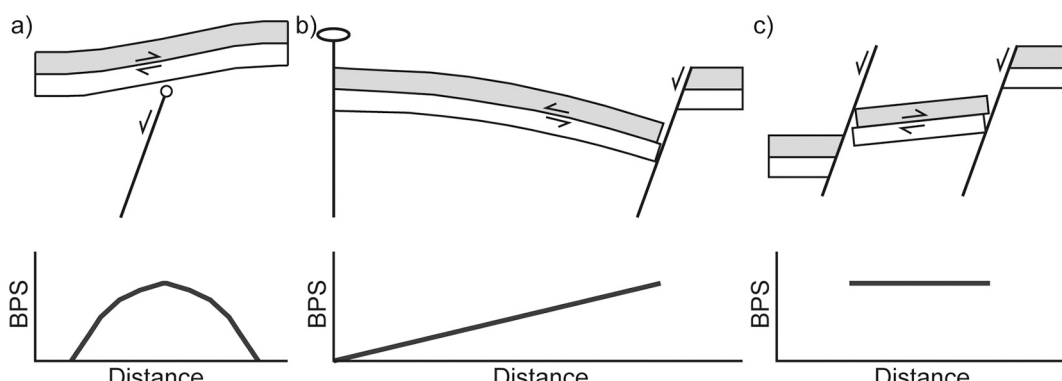


Fig. 13. Conceptual bed-parallel slip (BPS) profiles illustrating the expected distribution of slip due to (a) flexural-slip associated with fault propagation folding, (b) flexural-slip associated with hanging-wall rollover anticline, and (c) simple shear associated with bed rotations between interacting faults.

equivalent to the shear strain developed across a given layer (Ferrill et al., 2007). In this case, the prevailing bed thickness of ca. 1–2 m provides a slip of up to 0.63 m, an estimate which is close to the predicted BPS value of ca. 0.58–1.15 m.

Although the dip of the beds is likely to be a key control on the magnitude of BPS, there are some cases that it appears not to be the case. For example, the magnitude of BPS of up to 0.6 m along individual slip planes identified in the Lisan formation, cannot be related to high bed dips as in this case the bed dip is less than one degree (Weinberger et al., 2016). Nevertheless, BPS in this case is due to simple shear associated with co-seismic shaking, and our conceptual model is designed to make predictions of BPS magnitudes only for BPS due to flexural-slip folding and simple shear associated with bed rotations between interacting faults (Fig. 12).

5.3. Slip distribution along bed-parallel slip planes

In the previous section the range of BPS in extensional settings was discussed but without considering the spatial variations in BPS on individual planes. Delogkos et al. (2018) highlighted that the slip along individual BPS planes associated with flexural-slip is not constant, but instead varies from a maximum value approximately at the centre of the BPS plane to zero towards its tip. Fig. 9b shows a displacement profile along a ca. 500 m long BPS plane with a maximum slip of 2.9 m progressively decreasing towards the lateral tips. From a relatively limited range of slip magnitudes this study also highlighted a positive correlation between the maximum slip and length of BPS planes, with a slip to length ratio of ca. 0.016 falling within the range of the published values for other types of faults (e.g., Kim et al., 2004).

The notion of variable slip along BPS planes (e.g., Fig. 13a and b) is

consistent with observational constraints indicating that the overall magnitude of BPS varies with the dip of the bedding, as supported by data from the normal fault-related Big Brushy Canyon propagation fold (Fig. 9a). The same flexural-slip model was previously advocated in compressional settings where an increase in the slip magnitude typically occurs from the fold hinge to the limbs (Suppe, 1985; Tanner, 1989) and in extensional settings, associated with hanging-wall rollover anticlines, in which BPS increases from zero at the fold hinge, where the beds are pinned, to a maximum towards the master fault (Fig. 13b; Watterson et al., 1998). Whilst discontinuous BPS planes will usually reflect the changing boundary conditions from fold limbs to hinges, we also suggest that even within fold limbs with constant bed dips, BPS will be discontinuous, in the same way that other types of fractures are discontinuous, particularly at the early stages of fracture system evolution (Elliott, 1976; Walsh and Watterson, 1987). In other circumstances, the discontinuous nature of BPS may be very similar to that of segmented fault surfaces that are strongly kinematically linked, and may even be physically linked via relay structures, a scenario which is considered in the next section. By contrast, the magnitude of BPS due to the simple shear associated with bed rotations between interacting faults is expected to be constant along the BPS planes (Fig. 13c; Watterson et al., 1998) with an increase in magnitude as the slip planes rotate (Watterson et al., 1998; Ferrill et al., 1998).

5.4. Segmented nature of the bed-parallel slip planes

BPS is often accommodated by zones of multiple slip planes (Wilson et al., 2009; Weinberger et al., 2016) where slip is partitioned and transferred between the different slip planes. An example of displacement transfer is illustrated in Fig. 14a where one metre of slip is

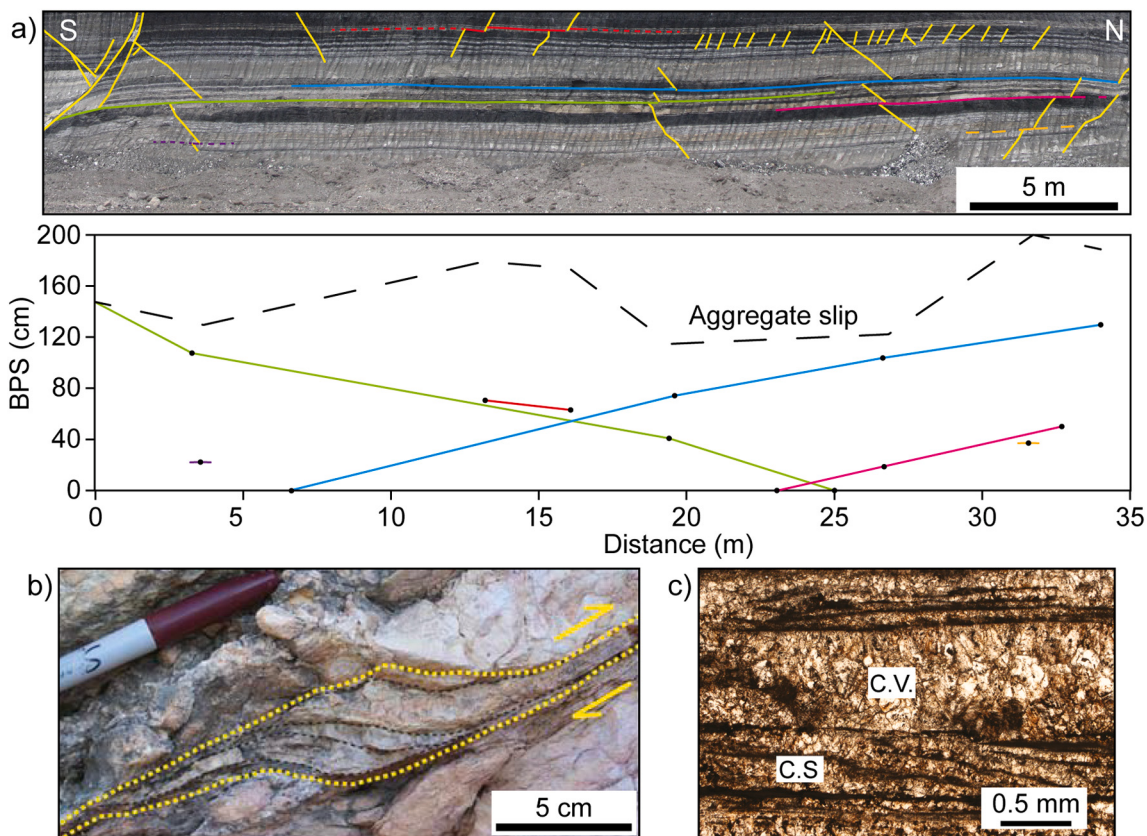


Fig. 14. (a) Outcrop photograph showing BPS planes that displace several normal faults and slip profiles along these BPS planes highlighting the displacement transfer between them and their segmented nature (modified after Delogkos et al., 2018). (b) Releasing step along a bed-parallel slip plane where calcite veins have filled rhombohedral or lenticular cavities produced by dilation (after Ferrill et al., 2007). (c) Details of microstructures within BPS planes highlighting shallow dipping veinlets in crack-seal veins. C.V. is calcite vein and C.S. is crack-seal vein (after Lemonnier et al., 2020).

transferred between two BPS planes (green and blue) that have a separation of ca. 1 m and an overlap of ca. 20 m (Delogkos et al., 2018). In this case, the BPS planes are segmented parallel to the slip direction but there are other cases where segmentation of the BPS planes is normal to the slip direction (e.g., Gross et al., 1997; Horne and Culshaw, 2001; Ferrill et al., 2007; Perritt and Roberts, 2007; Delogkos et al., 2018). As a consequence, in a similar fashion to faults (Walsh et al., 1999) depending on the relative slip direction and the sense of stepping, segmentation of the BPS planes can result in neutral (Figs. 1f and 15a), releasing (Figs. 1a, b and 15b) or restraining (Figs. 1e and 15c) relay zones. In the case of releasing relay zones, episodic slip and dilation can result in rhombohedral or lenticular veins filled by mineralisation and crack seals (e.g., Fig. 14b and c; Ferrill et al., 2007; Lemonnier et al., 2020).

The transfer of slip between the BPS planes can also be partly accommodated by minor normal faults which can be synthetic (Figs. 1b, 4a, c and bottom cartoon in 15b) or antithetic (Figs. 1a, 4d and top cartoon in 15b) to the BPS movement. Synthetic or ‘connecting’ normal faults are found to be associated with either neutral (Horne and Culshaw, 2001; Perritt and Roberts, 2007) or releasing relay zones (Gross et al., 1997; Ferrill et al., 2007; Delogkos et al., 2018). Antithetic or domino-style normal faults are found to be associated only with releasing relay zones (Delogkos et al., 2018). To our knowledge, there is no minor faulting (either synthetic or antithetic) associated with transfer of BPS in restraining relay zones. Finally, it is worth noting that the releasing relay zones appear to be much more common than restraining relays along the BPS planes in extensional settings (Ferrill et al., 2007; Delogkos et al., 2018), which is the opposite to what is observed for the BPS planes in contractional settings (Tanner, 1989, 1992; Horne and Culshaw, 2001).

5.5. Spatiotemporal distribution of bed-parallel slip

Our geometric models of BPS have considered constant bed thickness sequences associated with constant slip BPS planes (Section 5.2). These simplifying assumptions are useful insofar as they provide a means of estimating the potential scale of slip on planes that are a certain thickness apart. There are, however, compelling grounds for suggesting that the computed slips are best considered to relate to mechanical units, rather than individual beds, and that the spacing between BPS is neither uniform nor simple. For example, previous work has shown that multiple BPS planes can be spatially distributed and/or localised on a wide range of stratigraphic scales. Becker (1994) identified 8 BPS planes developed in association with fault propagation folding of a 550-m-thick Cretaceous sequence in the Ramon National Geological Park, Israel. At a much smaller scale, Weinberger et al. (2016) identified a zone of up to 11 BPS planes associated with co-seismic shaking, which can be continuously traced for more than 20 m and are localised within a metre-thick stratigraphic interval (average spacing of ca. 10 cm)

consisting of aragonite and detrital-rich layers of the Late Pleistocene Lisan Formation in the Dead Sea Basin. At an intermediate scale, Delogkos et al. (2018) reported that the distance between adjacent BPS planes ranges from a few centimetres up to 60 m with an average spacing of 13 m within the lignite/marl sequence in Ptolemais Basin, NW Greece. This evidence indicates that BPS are not distributed across all beds but are instead localised onto fewer planes presumably bounding discrete mechanical units. Whilst the localisation of BPS is likely to be controlled by a combination of bed thickness and mechanical stratigraphy, with slip localising preferentially on weaker layers bounding thicker and stronger units (e.g., Tanner, 1989; Higgs et al., 1991; Khalil and McClay, 2017), there are many other issues which will complicate any such relationship. It is anticipated, for example, that BPS could become stratigraphically more pervasive with time and increasing strain, with a decrease in the spacing of BPS planes accompanying the activation of new slip planes arising from fold tightening and progressive deformation. Evidence of equivalent decreases in spacing has been documented from earlier studies of BPS due to flexural-slip folding in contractional settings (Tanner, 1989; Fowler and Winsor, 1997; Horne and Culshaw, 2001). We suggest also that the segmented nature of BPS (see Section 5.4) demands that the spatial distribution of BPS within a rock volume will be highly variable in all directions (i.e., parallel and normal to slip direction) and will also vary with time as the segmented system localises. Another reason for expecting more complex arrangements of BPS is the kinematic interaction between BPS and normal faulting, an issue which is considered below (see Section 5.6).

5.6. Effects on magnitude, segmentation, and distribution of BPS due to the interaction with normal faulting

Thus far we have considered simple models for the distribution in BPS through a stratigraphic sequence, but without having considered the implications of their kinematic interaction. The distribution, spacing and magnitude of BPS is, however, likely to be strongly affected by the contemporaneous and mutually cross-cutting nature of BPS and normal faulting. Two main models have been advanced for the geometric and kinematic consequences of this interaction. In the conceptual model shown in Fig. 16a (Delogkos et al., 2018), pre-existing BPS planes (Stage 1) are displaced by normal faults (Stage 2), with subsequent reactivation of the BPS planes resulting in their lateral propagation and offset of the normal faults (Stage 3). The original distribution of the BPS planes has, therefore, been changed, with their final spacing partly depending on the throw of normal faults prior to reactivation of BPS. The net effect of this interaction is that the cumulative magnitude of BPS is eventually partitioned onto more BPS planes. Because this process can repeat several times (i.e., Stage 4), it can result in the clustering of what might originally have been regularly spaced BPS planes. This process is further complicated by the connectivity issues arising from the variable displacements across normal faults and BPS planes, which will provide

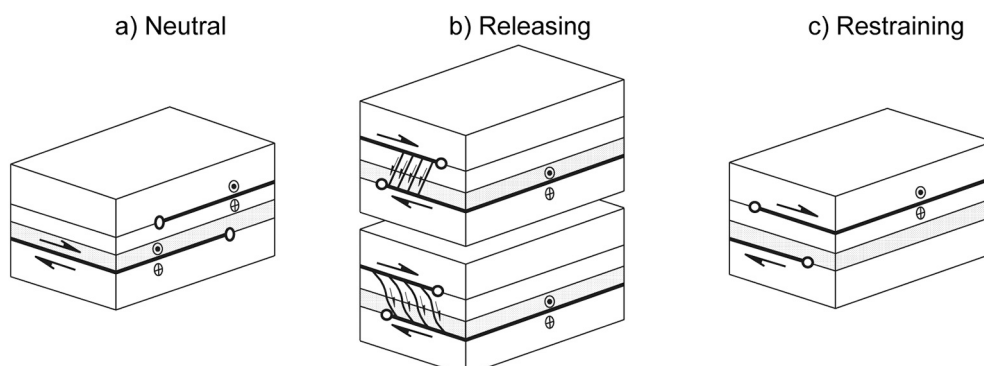


Fig. 15. Cartoons of neutral, releasing and restraining relay zones along bed-parallel slip planes in extensional settings (modified after Delogkos et al., 2018).

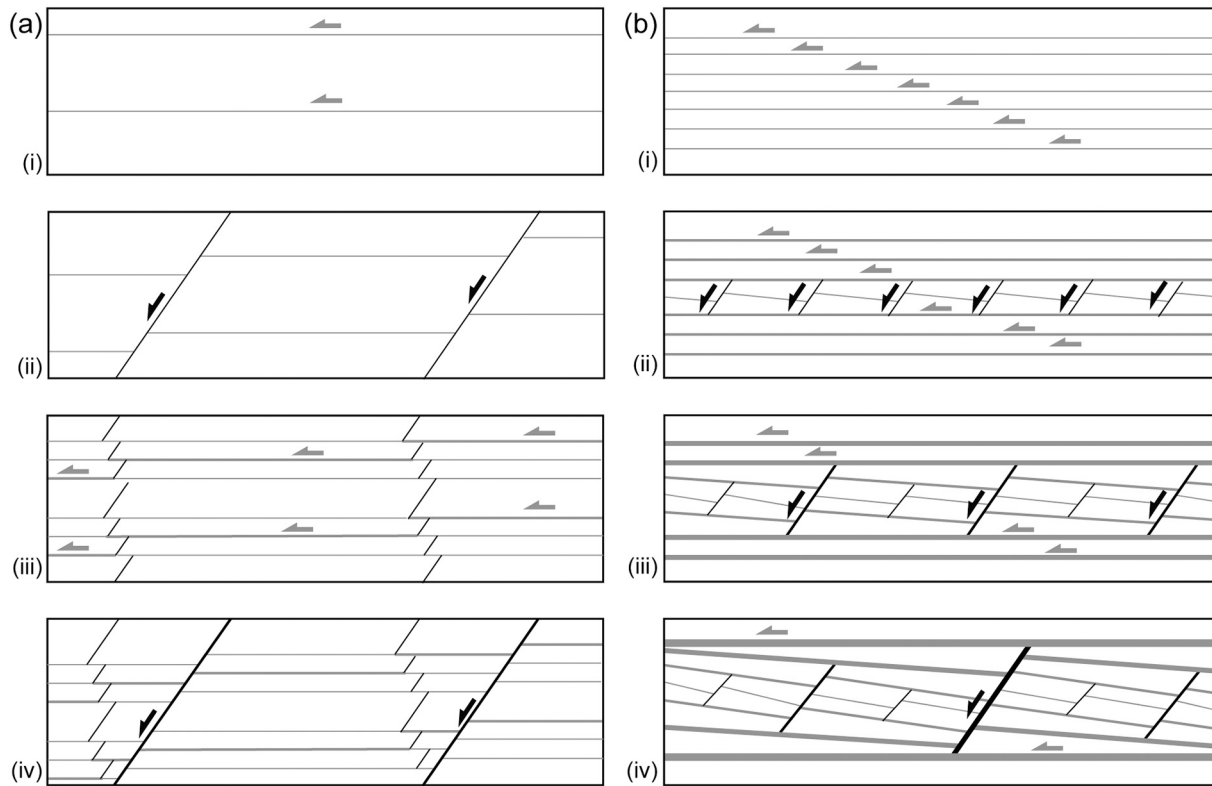


Fig. 16. Effects of interaction between BPS and normal faults on magnitude, segmentation, and distribution of bed-parallel slip. (a) Sequential illustration of their geometrical evolution during multiple repetitions of BPS and normal faulting modified after Delogkos et al. (2017), and (b) Sequential illustration of the relation between the zones of active BPS planes and block rotations modified after Gross et al. (1997). Slip initially is distributed throughout the section, eventually resulting in block rotation within individual beds. Due to the block rotation, several slip zones become inactive, resulting in localisation of the slip on less BPS planes above and below the rotating blocks. This tendency towards larger blocks and more widely spaced BPS planes continues in this manner.

even more complex geometries. These processes are considered to be partly responsible for the BPS clustering observed in the exposed sequence of Ptolemais FM, in Ptolemais Basin, NW Greece (Delogkos et al., 2018), for which outcrop examples and their associated geometric restorations (Fig. 16a) have been presented by Delogkos et al. (2017).

An alternative conceptual model for the distribution and magnitude of BPS planes is shown in Fig. 16b (Gross et al., 1997). In this case, however, contemporaneous normal faulting and associated block rotations provide a basis for localising BPS onto fewer and more widely spaced planes with time. BPS is initially distributed across numerous planes throughout the section (Stage 1). Strain accumulation leads to the formation of normal faulting between some of the BPS planes. These normal faults are kinematically related to the BPS planes, and therefore, they are abutted by them as described in Section 2.1. Furthermore, associated block rotation between the bounding BPS planes, in turn, leads to deactivation of the BPS planes that are displaced by the normal faults (Stage 2). BPS is then no longer accommodated by the planes located within these rotated blocks, but instead localised onto planes bounding these rotating blocks (Stage 3). This process of BPS localisation can gradually repeat at larger scales resulting in the development of larger rotated blocks, deactivation of associated BPS planes and wider spacing of the active BPS planes (Stage 4).

6. Discussion

In this section, we first discuss the potential for the widespread development of BPS within extensional settings despite the relatively limited attention they have received to date. We then explore the implications of our study and make suggestions for future research.

6.1. How common is bed-parallel slip in extensional settings?

The most common origin of BPS in extensional settings is the flexural-slip folding (Table 1). Given that deformation due to movement on normal faults is commonly accommodated partly by folding of the strata surrounding the faults, we would expect BPS to exist where any form of folding in extensional settings occurs. The examples of BPS identified in this study are associated with fault propagation and fault-bend folding, and the formation of hanging-wall rollover anticlines (Table 1). Seismic reflection and outcrop-based studies have, however, identified a wide variety of fold types associated with normal faulting, with the folds displaying various orientations, amplitudes and wavelengths relative to normal fault planes. We would therefore expect BPS to occur in association with fault-bend folding (e.g., Grosshong Jr, 1989; Withjack and Schlische, 2006; Delogkos et al., 2020; McHarg et al., 2020), normal and reverse drag folds (e.g., Hamblin, 1965; Barnett et al., 1987; Doutsos and Koukouvelas, 1998; Grasemann et al., 2005), including footwall anticlines and hanging-wall synclines associated with the along-strike variations in fault displacement (e.g., Schlische, 1995) and salt-related folding (e.g., Rowan et al., 2020). The fact that there are very few accounts within the published literature of BPS associated with folding is, however, attributed to observational bias arising from the paucity of steeply dipping markers that can highlight their presence.

The steepening of bed dips associated with fault zones and relay zones also provides an important basis for the generation of BPS. Bed rotations within fault-bounded zones can provide bed dips in excess of 45°, with relay ramps accommodating bed rotations of up to 30° prior to relay breaching. In many basins these deformations may not be as aerially extensive as flexural-slip folding, but they can lead to high shear strains of the intervening sequences and provide an excellent means of localising BPS. Whilst definition of BPS can, in this case, sometimes be

defined by the mutual offsetting of faults and BPS, recognition of its significance and scale is complicated by the associated complexity of structure and requires excellent outcrop constraints, where possible complemented by numerical modelling (e.g., Imber et al., 2004).

In terms of the nature of the host rock sequence that BPS would be expected to occur within, BPS is often identified in stratigraphic sequences with a strong mechanical contrast (Table 1), with a clear tendency of BPS to be predominantly accommodated by weak layers, independently of its origin (Salehy et al., 1977; Ferrill et al., 1998, 2007; Jackson et al., 2006). For example, Higgs et al. (1991) identified BPS planes within the mudstone horizon of a bedded unit comprising interbedded mudstones and sandstones of the Triassic Moenkopi Formation, associated with a hanging-wall rollover anticline. Khalil and McClay (2017) described BPS planes in incompetent thin-bedded shale dominated units associated with fault-propagation folding. The preferential location of BPS in weak units has also been attributed to the anisotropic properties of these layers that can promote slip parallel to the bedding (e.g., Ferrill et al., 1998). Alsop et al. (2020) highlighted that the location of BPS can also be controlled by the presence of competent or gypsum-rich units that have the ability to trap underlying fluids resulting in the localisation of the BPS planes directly beneath them. However, BPS has also been identified in relatively mechanically homogeneous sequences. Delogkos et al. (2017 and 2018) identified numerous BPS planes in a uniformly weak and relatively homogeneous sequence consisting of rhythmic alternations of m-scale lignite and lacustrine marl beds, and they suggested that the lack of significant mechanical heterogeneity is consistent with an even distribution of BPS through the exposed section.

In summary, BPS is expected to exist in all multi-layered host rock sequences, irrespective of their lithological and mechanical properties, and in the presence of any form of flexural-slip folding, tectonic or gravity-driven downslope movements, and associated with simple shear associated with either bed rotations between interacting faults or coseismic shaking. Its identification might, however, be challenging due to the nature of the host rock sequence, the scale and resolution of both outcrop and seismic reflection data, and the absence of suitable slip markers.

6.2. Implications and suggestions for further research

The development of BPS within normal fault systems has important implications for the manner in which deformation is accommodated and partitioned in extensional settings (e.g., Watterson et al., 1998; Ferrill et al., 2007; Delogkos et al., 2018; Alsop et al., 2020). This review indicates that bed rotations arising from deformation associated with normal faulting, such as the folding and shearing of adjacent host rock sequences, are accommodated by mm- to decametre scale BPS. In addition to large-scale normal faulting, tectonic stretching in the upper brittle crust can also be accommodated by other structures including fracturing, folding and a broad range of smaller normal faults, all of which promote the development of BPS.

Conceptual models of BPS development suggest that thin-bedded sequences will contain more smaller displacement BPS, with larger displacement BPS localised adjacent to thicker more massive units and providing greater mechanical decoupling of cross-cutting faults. Although of subordinate nature compared to associated normal fault displacements, BPS are nevertheless capable of transecting normal fault systems and introducing complexities in both fault zone structure and host rock deformation. Contemporaneous movement on faults and BPS will generate mutually intersecting structures which over protracted periods of time will form more complex and yet kinematically coherent fracture systems. These will, in turn, provide more complex host rock volumes and fracture arrays for subsurface flow, (e.g., Couples et al., 1998; Dholakia et al., 1998; Medici et al., 2016; Yuan et al., 2018) circumstances which make greater demands on the characterisation of fault-BPS systems and the prediction of associated fluid flow, and

potentially for a better estimation of the seismic hazard assessment. Published studies in contractional settings have demonstrated the potential of BPS planes to rupture during earthquakes, with active BPS planes accommodating a significant fraction of the total slip including coseismically produced geomorphic scarps (e.g., Philip and Meghraoui, 1983; Kelsey et al., 2008; Li et al., 2015; Otsubo et al., 2020).

Although the effects of BPS in extensional settings can be significant, there are not many studies providing detailed constraints on their development, a situation we attribute to their relatively small scale and to the paucity or absence of appropriate high angle structures highlighting their displacements. We also suspect that their illusive nature partly arises from our failure to recognise, or perhaps acknowledge, their potential significance and the prevalence of models that do not include BPS. Many aspects of their geometry and kinematics have yet to be investigated and future studies, based on well-suited outcrop/seismic reflection data and/or analogue/numerical modelling, should provide valuable knowledge on the role of structural configuration, mechanical stratigraphy, formation depth and prevailing fluid pressures on the initiation, development, and distribution of BPS within rock volumes. Only then can the implications of BPS for a variety of practical purposes be adequately defined.

7. Concluding remarks

1. This study compiles a global database of bed-parallel slip (BPS) associated with normal fault systems from 43 datasets derived from outcrop ($n = 38$), seismic reflection ($n = 2$), borehole ($n = 2$) and analogue sandbox ($n = 1$) studies.
2. BPS appears to be a common feature within multi-layered host rock sequences in extensional settings.
3. BPS within extensional basins is often found to be geometrically and/or kinematically associated with normal faulting.
4. The four main configurations identified in the literature between BPS and normal faulting are: (a) normal fault abutting BPS, (b) BPS abutting normal fault, (c) BPS offsetting normal fault, and (d) normal fault offsetting BPS.
5. The development of BPS is kinematically associated with a broad range of fault-related deformation, including bed rotations, flexural-slip folding, and both tectonic and gravity-driven sliding.
6. In our compiled global dataset, BPS typically ranges from a few millimetres up to 4.5 m, and is of the same order for all different origins of BPS.
7. For flexural-slip folding and simple shear models the magnitude of BPS is expected to have a linear relationship with bed thickness for a constant bed rotation angle, and with bed rotation angle for a constant bed thickness.
8. BPS is often accommodated by zones of multiple slip planes where slip is partitioned and transferred between the different slip planes.
9. The distribution of slip along the BPS planes is expected to differ depending on the origin of BPS.
10. Identification of BPS is often challenging due to its localised nature within bedded host rock sequences, the absence of suitable slip markers, and the scale and resolution of both outcrop and seismic reflection data.

Declaration of Competing Interest

The authors declare that they have no known competing financial interests or personal relationships that could have appeared to influence the work reported in this paper.

Acknowledgments

This research has been supported in part by a research grant from Science Foundation Ireland (SFI) and cofounded under the European

Regional Development Fund and by PIPCO RSG and its member companies (grant no. 13/RC/2092). This project has received funding from the Irish Research Council under grant number GOIPD/2020/530, and the European Union's Horizon 2020 research and innovation programme under the Marie Skłodowska-Curie grant agreement No 884931. Field observations in Utah and Kilve were made during the course of a consortium-sponsored project brokered by the Industry Technology Facilitator, and funded by Anadarko, ConocoPhillips (UK), Eni, ExxonMobil, Marathon Oil Corporation, Shell (UK), Equinor, Total E&P UK and Woodside Energy. Thanks to David Iacopini for providing further information about the seismic image in Fig. 11 which is available through the Virtual Seismic Atlas. Carlos Giraldo is thanked for permission to use the photograph in Fig. 6f. Thanks to the other members of the Fault Analysis Group and Giovanni Camanni for field assistance and useful discussions. We thank one anonymous reviewer, Kevin Smart and Bob Holdsworth for their useful comments and Carlo Doglioni for editorial handling.

References

- Alsop, G.I., Marco, S., 2011. Soft-sediment deformation within seismogenic slumps of the Dead Sea Basin. *J. Struct. Geol.* 33 (4), 433–457.
- Alsop, G.I., Weinberger, R., Marco, S., Levi, T., 2020. Bed-parallel slip: Identifying missing displacement in mass transport deposits. *J. Struct. Geol.* 131, 103952.
- Anderson, E.M., 1905. The dynamics of faulting. *Trans. Edinb. Geol. Soc.* 8, 387–402.
- Andrić, N., Matenco, L., Hilgen, F., de Bresser, H., 2018. Structural controls on sedimentation during asymmetric extension: the case of Sorbas Basin (SE Spain). *Glob. Planet. Chang.* 171, 185–206.
- Barnett, J.A., Mortimer, J., Rippon, J.H., Walsh, J.J., Watterson, J., 1987. Displacement geometry in the volume containing a single normal fault. *AAPG Bull.* 71 (8), 925–937.
- Bayrakci, G., Minshull, T.A., Sawyer, D., Reston, T.J., Klaeschen, D., Papenberg, C., Ranero, C., Bull, J., Davy, R., Shillington, D., Pérez-Gussinyé, M., 2016. Fault-controlled hydration of the upper mantle during continental rifting. *Nat. Geosci.* 9 (5), 384–388.
- Becker, A., 1994. Bedding-plane slip over a pre-existing fault, an example: the Ramon Fault, Israel. *Tectonophysics* 230 (1–2), 91–104.
- Benedicto, A., Schultz, R.A., 2010. Stylolites in limestone: magnitude of contractional strain accommodated and scaling relationships. *J. Struct. Geol.* 32 (9), 1250–1256.
- Bull, S., Cartwright, J., Huuse, M., 2009. A review of kinematic indicators from mass-transport complexes using 3D seismic data. *Mar. Pet. Geol.* 26 (7), 1132–1151.
- Carmignani, L., Kligfield, R., 1990. Crustal extension in the Northern Apennines: the transition from compression to extension in the Alpi Apuane core complex. *Tectonics* 9 (6), 1275–1303.
- Chapple, W.M., Spang, J.H., 1974. Significance of layer-parallel slip during folding of layered sedimentary rocks. *Geol. Soc. Am. Bull.* 85 (10), 1523–1534.
- Chigira, M., Tsou, C.Y., Matsushii, Y., Hiraiishi, N., Matsuzawa, M., 2013. Topographic precursors and geological structures of deep-seated catastrophic landslides caused by Typhoon Talas. *Geomorphology* 201, 479–493.
- Childs, C., Walsh, J.J., Watterson, J., 1990. A method for estimation of the density of fault displacements below the limits of seismic resolution in reservoir formations. In: Buller, A.T., et al. (Eds.), North Sea Oil and Gas Reservoirs II. Graham & Trotman, London, pp. 193–203.
- Childs, C., Watterson, J., Walsh, J.J., 1995. Fault overlap zones within developing normal fault systems. *J. Geol. Soc. Lond.* 152, 535–549.
- Childs, C., Watterson, J., Walsh, J.J., 1996. A model for the structure and development of fault zones. *J. Geol. Soc.* 153 (3), 337–340.
- Childs, C., Manzocchi, T., Nicol, A., Walsh, J.J., Soden, A.M., Conneally, J.C., Delogkos, E., 2017. The relationship between normal drag, relay ramp aspect ratio and fault zone structure. *Geol. Soc. Lond., Spec. Publ.* 439 (1), 355–372.
- Childs, C., Delogkos, E., Manzocchi, T., Walsh, J.J., 2020. A geological record of changing propagation directions of fault slip events during the growth of a normal fault system. *Tectonophysics* 774, 228296.
- Cobbold, P.R., Mourges, R., Boyd, K., 2004. Mechanism of thin-skinned detachment in the Amazon Fan: assessing the importance of fluid overpressure and hydrocarbon generation. *Mar. Pet. Geol.* 21 (8), 1013–1025.
- Coleman, A.J., Duffy, O.B., Jackson, C.A.L., 2019. Growth folds above propagating normal faults. *Earth Sci. Rev.* 196, 102885.
- Couples, G.D., Lewis, H., Tanner, P.G., 1998. Strain partitioning during flexural-slip folding. *Geol. Soc. Lond., Spec. Publ.* 127 (1), 149–165.
- Daniel, J.M., Moretti, I., Micarelli, L., Chuyne, S.E., Delle Piane, C., 2004. Macroscopic structural analysis of AG10 well (Gulf of Corinth, Greece). *Compt. Rendus Geosci.* 336 (4–5), 435–444.
- Delogkos, E., Childs, C., Manzocchi, T., Walsh, J.J., Pavlides, S., 2017. The role of bed-parallel slip in the development of complex normal fault zones. *J. Struct. Geol.* <https://doi.org/10.1016/j.jsg.2017.02.014>.
- Delogkos, E., Childs, C., Manzocchi, T., Walsh, J.J., 2018. The nature and origin of bed-parallel slip in Kardia mine, Ptolemais Basin, Greece. *J. Struct. Geol.* 113, 115–133. <https://doi.org/10.1016/j.jsg.2018.05.015>.
- Delogkos, E., Saqab, M.M., Walsh, J.J., Roche, V., Childs, C., 2020. Throw variations and strain partitioning associated with fault-bend folding along normal faults. *Solid Earth* 11, 935–945. <https://doi.org/10.5194/se-11-935-2020>.
- Dholakia, S.K., Aydin, A., Pollard, D.D., Zoback, M.D., 1998. Fault-controlled hydrocarbon pathways in the Monterey Formation, California. *AAPG Bull.* 82 (8), 1551–1574.
- Donath, F.A., 1961. Experimental study of shear failure in anisotropic rocks. *Geol. Soc. Am. Bull.* 72 (6), 985–989.
- Doutsos, T., Koukouvelas, I., 1998. Fractal analysis of normal faults in northwestern Aegean area, Greece. *J. Geodyn.* 26 (2–4), 197–216.
- Eisenstadt, G., De Paor, D.G., 1987. Alternative model of thrust-fault propagation. *Geology* 15 (7), 630–633.
- Elliott, D., 1976. The energy balance and deformation mechanisms of thrust sheets. *Phil. Trans. Roy. Soc. Lond. A* 283, 289–312.
- Fagereng, Å., Byrnes, G., 2015. A range of fault slip styles on progressively misoriented planes during flexural-slip folding, Cape Fold Belt, South Africa. *J. Struct. Geol.* 70, 156–169.
- Ferrill, D.A., Morris, A.P., Jones, S.M., Stamatakos, J.A., 1998. Extensional layer-parallel shear and normal faulting. *J. Struct. Geol.* 20 (4), 355–362.
- Ferrill, D.A., Morris, A.P., Smart, K.J., 2007. Stratigraphic control on extensional fault propagation folding: big Brushy Canyon monocline, Sierra del Carmen, Texas. *Geol. Soc. Lond., Spec. Publ.* 292 (1), 203–217.
- Ferrill, D.A., Morris, A.P., McGinnis, R.N., 2009. Crossing conjugate normal faults in field exposures and seismic data. *AAPG Bull.* 93 (11), 1471–1488.
- Ferrill, D.A., Morris, A.P., McGinnis, R.N., 2012a. Extensional fault-propagation folding in mechanically layered rocks: the case against the frictional drag mechanism. *Tectonophysics* 576, 78–85.
- Ferrill, D.A., McGinnis, R.N., Morris, A.P., Smart, K.J., 2012b. Hybrid failure: Field evidence and influence on fault refraction. *J. Struct. Geol.* 42, 140–150.
- Fossen, H., 2020. Fault classification, fault growth and displacement. In: *Regional Geology and Tectonics: Principles of Geologic Analysis*. Elsevier, pp. 119–147. <https://doi.org/10.1016/b978-0-444-64134-2.00007-9>.
- Fowler, T.J., 1996. Flexural-slip generated bedding-parallel veins from Central Victoria, Australia. *J. Struct. Geol.* 18 (12), 1399–1415.
- Fowler, T.J., Winsor, C.N., 1997. Characteristics and occurrence of bedding-parallel slip surfaces and laminated veins in chevron folds from the Bendigo-Castlemaine goldfields: implications for flexural-slip folding. *J. Struct. Geol.* 19 (6), 799–815.
- Gamboa, D., Alves, T.M., 2015. Three-dimensional fault meshes and multi-layer shear in mass-transport blocks: implications for fluid flow on continental margins. *Tectonophysics* 647, 21–32.
- Gawthorpe, R.L., Sharp, I., Underhill, J.R., Gupta, S., 1997. Linked sequence stratigraphic and structural evolution of propagating normal faults. *Geology* 25 (9), 795–798.
- Gibbs, A.D., 1984. Structural evolution of extensional basin margins. *J. Geol. Soc.* 141 (4), 609–620.
- Gillespie, P.A., Howard, C.B., Walsh, J.J., Watterson, J., 1993. Measurement and characterisation of spatial distributions of fractures. *Tectonophysics* 226, 113–141.
- Granado, P., Tavani, S., Carrera, N., Muñoz, J.A., 2018. Deformation pattern around the conejera fault blocks (asturian basin, north iberian margin). *Geol. Acta* 16 (4), 357–373.
- Grasemann, B., Martel, S., Passchier, C., 2005. Reverse and normal drag along a fault. *J. Struct. Geol.* 27 (6), 999–1010.
- Groshong Jr., R.H., 1989. Half-graben structures: Balanced models of extensional fault-bend folds. *Geol. Soc. Am. Bull.* 101 (1), 96–105.
- Gross, M.R., Becker, A., Gutiérrez-Alonso, G., 1997. Transfer of displacement from multiple slip zones to a major detachment in an extensional regime: example from the Dead Sea rift, Israel. *Geol. Soc. Am. Bull.* 109 (8), 1021–1035.
- Gutiérrez, F., Carbonell, D., Kirkham, R.M., Guerrero, J., Lucha, P., Matthews, V., 2014. Can flexural-slip faults related to evaporite dissolution generate hazardous earthquakes? The case of the Grand Hogback monocline of west-Central Colorado. *Bulletin* 126 (11–12), 1481–1494.
- Hamblin, W.K., 1965. Origin of “reverse drag” on the downthrown side of normal faults. *Geol. Soc. Am. Bull.* 76 (10), 1145–1164.
- Hancock, P.L., 1985. Brittle microtectonics: principles and practice. *J. Struct. Geol.* 7 (3–4), 437–457.
- Healy, D., 2009. Anisotropy, pore fluid pressure and low angle normal faults. *J. Struct. Geol.* 31 (6), 561–574.
- Higgs, W., Williams, G., Powell, C., 1991. Evidence for flexural shear folding associated with extensional faults. *Geol. Soc. Am. Bull.* 103 (5), 710–717.
- Horne, R., Culshaw, N., 2001. Flexural-slip folding in the Meguma group, Nova Scotia, Canada. *J. Struct. Geol.* 23 (10), 1631–1652.
- Hubbert, M.K., Rubey, W.W., 1959. Role of fluid pressure in mechanics of overthrust faulting: i. Mechanics of fluid-filled porous solids and its application to overthrust faulting. *Geol. Soc. Am. Bull.* 6, 115–166.
- Iacopini, D., Butler, R.W.H., Purves, S., McArdle, N., De Freslon, N., 2016. Exploring the seismic expression of fault zones in 3D seismic volumes. *J. Struct. Geol.* 89, 54–73.
- Imber, J., Tuckwell, G.W., Childs, C., Walsh, J.J., Heath, A., Manzocchi, T., Bonson, C.G., Strand, J.A., 2004. 3-D distinct element modelling of relay growth and breaching along normal faults. *J. Struct. Geol.* 26, 1897–1911.
- Ishii, E., 2016. The role of bedding in the evolution of meso-and microstructural fabrics in fault zones. *J. Struct. Geol.* 89, 130–143.
- Jackson, J.A., 1987. Active normal faulting and crustal extension. In: Coward, M.P., Dewey, J.F., Hancock, P.L. (Eds.), *Continental Extensional Tectonics, Special Publication*, vol. 28. Geological Society, London, pp. 3–17.

- Jackson, C.A.L., Gawthorpe, R.L., Sharp, I.R., 2006. Style and sequence of deformation during extensional fault-propagation folding: examples from the Hammam Faraun and El-Qaa fault blocks, Suez Rift, Egypt. *J. Struct. Geol.* 28 (3), 519–535.
- Kakimi, T., 1980. Magnitude-frequency relation for displacement of minor faults and its significance in crustal deformation. *Bull. Geol. Surv. Jpn.* 31, 467–487.
- Kelsey, H.M., Sherrod, B.L., Nelson, A.R., Brocher, T.M., 2008. Earthquakes generated from bedding plane-parallel reverse faults above an active wedge thrust, Seattle fault zone. *Geol. Soc. Am. Bull.* 120 (11–12), 1581–1597.
- Khalil, S.M., McClay, K.R., 2017. 3D geometry and kinematic evolution of extensional fault-related folds, NW Red Sea, Egypt. *Geol. Soc. Lond., Spec. Publ.* 439 (1), 109–130.
- Khanlari, G., Rafiee, B., Abdilor, Y., 2015. Evaluation of strength anisotropy and failure modes of laminated sandstones. *Arab. J. Geosci.* 8 (5), 3089–3102.
- Kim, Y.S., Peacock, D.C., Sanderson, D.J., 2004. Fault damage zones. *J. Struct. Geol.* 26 (3), 503–517.
- Korneva, I., Tondi, E., Balsamo, F., Agosta, F., 2016. Deformation mechanisms and petrophysical properties of chert and limestone fault rocks within slope-to-basin succession (Gargano Promontory, Southern Italy). *Tectonophysics* 690, 52–62.
- Lansigu, C., Bouroullec, R., 2004. Staircase normal fault geometry in the Grès d'Annot (SE France). *Geol. Soc. Lond., Spec. Publ.* 221 (1), 223–240.
- Laubach, S.E., Hundley, T.H., Hooker, J.N., Marrett, R.A., 2018. Spatial arrangement and size distribution of normal faults, Buckskin Detachment upper plate, Western Arizona. *J. Struct. Geol.* 108, 230–242.
- Lemonnier, N., Homberg, C., Roche, V., Rocher, M., Schnyder, J., 2020. Microstructures of bedding-parallel faults under multistage deformation: examples from the Southeast Basin of France. *J. Struct. Geol.* 104138.
- Li, T., Chen, J., Thompson, J.A., Burbank, D.W., Yang, X., 2015. Active flexural-slip faulting: a study from the Pamir-Tian Shan convergent zone, NW China. *J. Geophys. Res. Solid Earth* 120 (6), 4359–4378.
- Lymer, G., Cresswell, D.J., Reston, T.J., Bull, J.M., Sawyer, D.S., Morgan, J.K., Stevenson, C., Causer, A., Minshull, T.A., Shillington, D.J., 2019. 3D development of detachment faulting during continental breakup. *Earth Planet. Sci. Lett.* 515, 90–99.
- McHarg, S., Elders, C., Cunneen, J., 2020. Extensional fault-related folding of the North West shelf, Western Australia. *AAPG Bull.* 104 (4), 913–938.
- Medici, G., West, L.J., Mountney, N.P., 2016. Characterizing flow pathways in a sandstone aquifer: tectonic vs sedimentary heterogeneities. *J. Contam. Hydrol.* 194, 36–58.
- Morley, C.K., 2014. Outcrop examples of soft-sediment deformation associated with normal fault terminations in Deepwater, Eocene turbidites: a previously undescribed conjugate fault termination style? *J. Struct. Geol.* 69, 189–208.
- Morris, A., Ferrill, D.A., Henderson, D.B., 1996. Slip-tendency analysis and fault reactivation. *Geology* 24 (3), 275–278.
- Nabavi, S.T., Alavi, S.A., Wibberley, C.A., Jahangiri, M., 2020. Normal fault networks and their spatial relationships in Plio-Quaternary sedimentary series: a case study in the Zanjan Depression, NW Iran. *J. Struct. Geol.* 104072.
- Niandou, H., Shao, J.F., Henry, J.P., Fourmaux, D., 1997. Laboratory investigation of the mechanical behaviour of Tournemire shale. *Int. J. Rock Mech. Min. Sci.* 34 (1), 3–16.
- Otsubo, M., Katayama, I., Miyakawa, A., Sagiya, T., 2020. Inelastic behavior and mechanical strength of the shallow upper crust controlled by layer-parallel slip in the high-strain zone of the Niigata region, Japan. *Earth Planets Space* 72 (1), 1–7.
- Peacock, D.C.P., Sanderson, D.J., 1991. Displacements, segment linkage and relay ramps in normal fault zones. *J. Struct. Geol.* 13 (6), 721–733.
- Peacock, D.C.P., Kniipe, R.J., Sanderson, D.J., 2000. Glossary of normal faults. *J. Struct. Geol.* 22 (3), 291–305.
- Pedrera, A., Galindo-Zaldívar, J., Lamas, F., Ruiz-Constán, A., 2012. Evolution of near-surface ramp-flat-ramp normal faults and implication during intramontane basin formation in the eastern Betic Cordillera (the Huécar-Oveira Basin, SE Spain). *Tectonics* 31 (4).
- Perritt, S., Roberts, M., 2007. Flexural-slip structures in the bushveld complex, South Africa? *J. Struct. Geol.* 29 (9), 1422–1429.
- Philip, H., Meghraoui, M., 1983. Structural analysis and interpretation of the surface deformations of the El Asnam earthquake of October 10, 1980. *Tectonics* 2 (1), 17–49.
- Price, N.J., Cosgrove, J.W., 1990. Analysis of Geological Structures. Cambridge University Press, p. 502.
- Proffett Jr., J.M., 1977. Cenozoic geology of the Yerington district, Nevada, and implications for the nature and origin of Basin and Range faulting. *Geol. Soc. Am. Bull.* 88 (2), 247–266.
- Ramsay, J.G., 1974. Development of chevron folds. *Geol. Soc. Am. Bull.* 85 (11), 1741–1754.
- Ramsay, J.G., 1980. Shear zone geometry: a review. *J. Struct. Geol.* 2 (1–2), 83–99.
- Ramsey, J.M., Chester, F.M., 2004. Hybrid fracture and the transition from extension fracture to shear fracture. *Nature* 428 (6978), 63–66.
- Reston, T.J., 2005. Polyphase faulting during the development of the wet Galicia rifted margin. *Earth Planet. Sci. Lett.* 237, 561–576.
- Rich, J.L., 1934. Mechanics of low-angle overthrust faulting as illustrated by Cumberland thrust block, Virginia, Kentucky, and Tennessee. *AAPG Bull.* 18 (12), 1584–1596.
- Roche, V., Homberg, C., Rocher, M., 2012. Fault displacement profiles in multilayer system: from fault restriction to fault propagation. *Terra Nova*. <https://doi.org/10.1111/j.1365-3121.2012.01088.x>.
- Roche, V., Homberg, C., van der Baan, M., Rocher, M., 2017. Widening of normal fault zones due to the inhibition of vertical propagation. *Geol. Soc. Lond. Spec. Publ.* 439 (1), 271–288.
- Rowan, M.G., Kligfield, R., 1989. Cross section restoration and balancing as aid to seismic interpretation in extensional terranes. *AAPG Bull.* 73 (8), 955–966.
- Rowan, M.G., Muñoz, J.A., Giles, K.A., Roca, E., Hearon IV, T.E., Fiduk, J.C., Ferrer, O., Fischer, M.P., 2020. Folding and fracturing of rocks adjacent to salt diapirs. *J. Struct. Geol.* 104187.
- Salehy, M.R., Money, M.S., Dearman, W.R., 1977. The occurrence and engineering properties of intraformational shears in Carboniferous rocks. In: Proceedings Conference Rock Engineering, Newcastle-upon-Tyne, pp. 311–328.
- Sanderson, D., 1982. Models of strain variation in nappes and thrust sheets: a review. *Tectonophysics* 88 (3–4), 201–233.
- Sanderson, D., Manchini, W., 1984. Transpression. *J. Struct. Geol.* 6, 449–458.
- Schlische, R.W., 1995. Geometry and origin of fault-related folds in extensional settings. *AAPG Bull.* 79 (11), 1661–1678.
- Séjourné, S., Malo, M., Savard, M.M., Kirkwood, D., 2005. Multiple origin and regional significance of bedding parallel veins in a fold and thrust belt: the example of a carbonate slice along the Appalachian structural front. *Tectonophysics* 407 (3–4), 189–209.
- Sharp, I.R., Gawthorpe, R.L., Underhill, J.R., Gupta, S., 2000. Fault-propagation folding in extensional settings: examples of structural style and synrift sedimentary response from the Suez rift, Sinai, Egypt. *Geol. Soc. Am. Bull.* 112 (12), 1877–1899.
- Shaw, J.H., Suppe, J., 1994. Active faulting and growth folding in the eastern Santa Barbara Channel, California. *Geol. Soc. Am. Bull.* 106 (5), 607–626.
- Shelton, J.W., 1984. Listric normal faults: an illustrated summary. *AAPG Bull.* 68 (7), 801–815.
- Sibson, R.H., 2000. Fluid involvement in normal faulting. *J. Geodyn.* 29 (3–5), 469–499.
- Smart, K.J., Ferrill, D.A., Morris, A.P., Bichon, B.J., Riha, D.S., Huyse, L., 2010. Geomechanical modeling of an extensional fault-propagation fold: big Brushy Canyon monocline, Sierra Del Carmen, Texas. *AAPG Bull.* 94 (2), 221–240.
- Sobiesiak, M.S., Kneller, B., Alsop, G.I., Milana, J.P., 2018. Styles of basal interaction beneath mass transport deposits. *Mar. Pet. Geol.* 98, 629–639.
- Stein, R.S., King, G.C., Rundle, J.B., 1988. The growth of geological structures by repeated earthquakes 2. Field examples of continental dip-slip faults. *J. Geophys. Res. Solid Earth* 93 (B11), 13319–13331.
- Stimpson, B., Walton, G., 1970. September. Clay mylonites in English Coal Measures—their significance in opencast slope stability. In: First International Congress of the International Association of Engineering Geology, Paris, France, 8–11 September 1970, pp. 1388–1393 (Comité français de géologie de l'ingénieur).
- Suppe, J., 1985. Principles of Structural Geology. Prentice Hall.
- Tanner, P.G., 1989. The flexural-slip mechanism. *J. Struct. Geol.* 11 (6), 635–655.
- Tanner, P.G., 1992. Morphology and geometry of duplexes formed during flexural-slip folding. *J. Struct. Geol.* 14 (10), 1173–1192.
- Walsh, J.J., Watterson, J., 1987. Distributions of cumulative displacement and seismic slip on a single normal fault surface. *J. Struct. Geol.* 9, 1039–1046.
- Walsh, J.J., Watterson, J., Bailey, W.R., Childs, C., 1999. Fault Relays, Bends and Branchlines. *J. Struct. Geol.* 21, 1019–1026.
- Watterson, J., Childs, C., Walsh, J.J., 1998. Widening of fault zones by erosion of asperities formed by bed-parallel slip. *Geology* 26 (1), 71–74.
- Weinberger, R., Levi, T., Alsop, G.I., Eyal, Y., 2016. Coseismic horizontal slip revealed by sheared clastic dikes in the Dead Sea Basin. *Bulletin* 128 (7–8), 1193–1206.
- Wibberley, C.A., Petit, J.P., Rives, T., 2007. The effect of tilting on fault propagation and network development in sandstone-shale sequences: a case study from the Lodève Basin, southern France. *J. Geol. Soc.* 164 (3), 599–608.
- Wilson, P., Gawthorpe, R.L., Hodgetts, D., Rarity, F., Sharp, I.R., 2009. Geometry and architecture of faults in a syn-rift normal fault array: the Nukhul half-graben, Suez rift, Egypt. *J. Struct. Geol.* 31 (8), 759–775.
- Withjack, M.O., Schlische, R.W., 2006. Geometric and experimental models of extensional fault-bend folds. *Geol. Soc. Lond., Spec. Publ.* 253 (1), 285–305.
- Withjack, M.O., Olson, J., Peterson, E., 1990. Experimental models of extensional forced folds. *AAPG Bull.* 74 (7), 1038–1054.
- Wojtal, S., 1986. Deformation within foreland thrust sheets by populations of minor faults. *J. Struct. Geol.* 8, 341–360.
- Ye, Qing, Mei, Lianfu, Jiang, Dapeng, Xu, Xinming, Delogkos, Efstratios, Zhang, Lili, Camanni, Giovanni, 2022. 3D structure and development of a metamorphic core complex in the northern South China Sea rifted margin. *J. Geophys. Res. Solid Earth* 127 (2), e2021JB022595. <https://doi.org/10.1029/2021JB022595>.
- Yuan, R.S., Schutjens, P.M.T.M., Bourgeois, F.G., Calvert, M.A., 2018. August. Fault slip or bed-parallel shear? A multi-scenario modeling approach to investigating well deformation in the deep overburden of a compacting reservoir in the North Sea. In: In 52nd US Rock Mechanics/Geomechanics Symposium. American Rock Mechanics Association.
- van der Zee, W., Wibberley, C.A., Urai, J.L., 2008. The influence of layering and pre-existing joints on the development of internal structure in normal fault zones: the Lodève basin, France. *Geol. Soc. Lond., Spec. Publ.* 299 (1), 57–74.